



Master's thesis

**Numerical implementation of a new
gravitational force derived within
Spacetime Algebra**

Irati Lizaso Berrueta

Supervisor: Steen H. Hansen

Submitted: July 3, 2023

Acknowledgement

I would like to thank my supervisor Steen Hansen for sharing the beautiful framework of spacetime algebra with me. Although hard and occasionally frustrating, this has been an undoubtedly enlightening journey that has completely changed the way I see geometry.

Abstract

Spacetime Algebra (STA) has proved to be a powerful tool for the study of a number of physics' theories. Many concepts in physics arise naturally from its geometric structure, which allows a simple and coordinate-free formulation of physics. Motivated by its uncomplicated description of the electromagnetic theory, in this work we derive a gravitational force within this framework, which consists of a Newtonian term and an additional $\vec{v} \times \vec{L}$ term, and implement it on 200 test particles orbiting around the Milky Way.

By additionally implementing a standard Newtonian force, we compare the orbits generated by both forces and conclude that the extra term causes orbit precession. In this way, the STA formulation of gravity might prove advantageous over the Newtonian theory, given that it seems to be able to properly describe precession.

Contents

1	Introduction	1
2	Spacetime algebra	3
2.1	Geometric algebra	4
2.1.1	Geometric algebra in two dimensions	7
2.1.2	Geometric algebra in three dimensions	8
2.2	Spacetime algebra	11
2.2.1	Lorentz transformations	13
2.2.2	Spacetime split	14
2.3	Derivation of the gravitational force	16
2.3.1	Computation of \vec{N} and \vec{L}	19
3	Numerical implementation of the force	22
3.1	Simulation	22
3.1.1	Simulating the Milky Way	23
3.1.2	Generating the test particles	24
3.1.3	Orbit integration	25
3.1.4	Comparing the orbits	26
3.2	The effect of the $\vec{v} \times \vec{L}$ term	27
3.3	Discussion and further explorations	30
4	Conclusions	32
A	Conserved quantities within classical field theory	34
B	Numerical implementation	36
B.1	Hernquist potential	36
B.2	Leapfrog integrator	36
B.3	Additional figures	38
	Bibliography	42

Chapter 1

Introduction

The Milky Way has since bygone ages been a major source of interest. Marvelling at the immense band of white light traversing the sky, many thinkers would wonder about its origin, trying to answer two fundamental questions about it: what it was and why it was there. After a large number of hypotheses and with the development of improved telescopes, we eventually came to learn that what we saw in the sky was a rotating disk of stars, bound together by gravity, and that our Solar System was part of it. However, among these stars there were other bright bodies that did not follow their motion; these had a similar structure to that of the Milky Way, and we called them galaxies.

As the constituent elements of our Universe, galaxies have always played a central role in what we know about it. Some of the most fascinating breakthroughs of modern cosmology were in fact made by studying them, which shows the great value they hold as natural laboratories. In particular, we were able to postulate the existence of dark matter from examining galactic dynamics, and we found out that the Universe is expanding by observing galaxies' redshifts.

There are still many things that we can learn from studying galaxies. For example, there is a particularly intriguing discrepancy between standard cosmological predictions and observations regarding the Milky Way's satellite galaxies. According to our current cosmological paradigm, dwarf galaxies orbiting the Milky Way should be spherically distributed around it. However, a number of investigations [1, 2, 3] indicate that their orbits lie on a plane. In theory this could be due to statistical fluctuations, there is in fact a recent report [4] that argues that the plane of satellites could be transient and thus compatible with the standard cosmological model, but additional studies show that the Andromeda galaxy has a very similar structure [5], suggesting that the planar distribution of satellite galaxies might be related to cosmological causes.

In this project we will focus on the orbits of these dwarf galaxies around the Milky Way. Given that current simulations using the standard gravitational force are not able to reproduce their planar distribution, we are going to add a new term to the Newtonian force.

The suggested term, introduced in [6], is derived from *spacetime algebra* (STA), which is the geometric algebra of Minkowski spacetime $\mathcal{G}(\mathcal{M}^4)$ — or equivalently the Clifford algebra

$\mathcal{C}(1, 3)$. This framework was developed by the theoretical physicist David Hestenes in the second half of the 20th century, and has lately gained considerable attention due to its simple and straight-forward formulation of physics. In our current physical framework, a thorough understanding of many concepts and theories often requires one's familiarity with complex mathematical tools, which usually entail several limitations. A good example of this is the standard tensor algebra, which, apart from being essentially coordinate-based — and thus, significant effort needs to be put into proving covariance of quantities —, is highly restricted to the field of relativity theory; spins, for example, are not adequately described by tensors, and therefore require learning the completely different language of spinors. By changing the way we treat geometry, spacetime algebra allows a coordinate-free formulation of physics, as well as a uniform description of classical, quantum and relativistic physics. Thus, Hestenes introduced it as a unified mathematical framework that would provide a deeper understanding of physical concepts, making physics available to a wider range of students, for which he won the Ørsted award of teaching [7].

The formulation of electromagnetism within STA is specially interesting for our case. By combining the electric and magnetic fields into a single electromagnetic bivector field $\mathbf{F} = \vec{E} + \vec{B}I$, both Maxwell's equations and the Lorentz force appear naturally. The simplicity provided by this framework is made manifest in that Maxwell's equations are reduced to a single equation. Based on the electromagnetic case, we can similarly define an angular momentum bivector \mathbf{M} that combines the dynamic mass moment \vec{N} and the angular momentum \vec{L} as $\mathbf{M} = -c\vec{N} - \vec{L}I$, which will allow us to derive Maxwell's equations of gravity and a gravitational force that is equivalent to the Lorentz force. It is in this force that we find the new term, in addition to a Newtonian term.

The present work aims to study the effect of the new force term, which we will do by simulating the orbits of a number of randomly generated satellite galaxies around the Milky Way. These orbits will be computed using both the standard Newtonian force and the new gravitational force derived within spacetime algebra. We will then be able to analyze the effect of the additional term by comparing both simulations.

The work is divided into two main parts. We start with a detailed introduction to spacetime algebra in Chapter 2, where we build the specific tools we need in order to derive the gravitational force in the last section. Chapter 3 presents the numerical implementation of the force, with a description of the simulation and the discussion of the results, as well as suggestions for further explorations. Finally, some conclusions are drawn in the last chapter.

Chapter 2

Spacetime algebra

Fundamentally, a vector is a mathematical object characterized by its magnitude and its direction. Vector spaces generalize this concept by defining vector addition and scalar multiplication, but in order to describe geometry we also need to be able to work with distances and angles, which we can do by introducing an adequate multiplication rule for vectors.

One would instinctively think of the scalar product, as it introduces the concepts of length and orthogonality, but it has one significant limitation – it is not invertible. The fact that we have to project one vector into another means that we will be losing information on the way. The same can be said of the cross product; although we would now be generating a third vector instead of a bare scalar, it can be seen that for two perpendicular vectors \vec{a} and \vec{c} , there exist infinitely many vectors \vec{b} that satisfy $\vec{a} \times \vec{b} = \vec{c}$.

Developing a proper vector algebra is certainly not a trivial matter. In fact, the need to place geometry within a unified algebraic framework became a major concern for 19th century mathematics. The first attempt was made by the mathematician W. R. Hamilton with the discovery of quaternion formulation in 1843 [8], based on the multiplication between complex numbers. He wanted to generalize the unit imaginary i to more dimensions; given that complex numbers can be represented by two perpendicular axes on a plane, this would allow him to represent vectors in space by adding a third axis perpendicular to the other two. He found that one perpendicular axis representing a second complex number j was not enough to construct an adequate product – he still needed a third complex number, k . Thus, he introduced the expression $(a + ib + jc + kd)$ that he called a quaternion, where i, j and k satisfied $i^2 = j^2 = k^2 = -1$, and claimed that vectors could be represented by *pure* quaternions of the form $(ib + jc + kd)$. Multiplying two vectors would now give a scalar part and a vector part, leading to the definition of our familiar scalar and cross products. And this new quaternion product had a great advantage, since it turned out to be invertible. However, it was still not good enough. One problem was that the algebra did not close – the full product still had a scalar part despite coming from two pure vectors. Nevertheless, its major limitation was the impossibility to generalize it for arbitrary dimensions, because the cross product could only be defined in three dimensions.

It was Hermann Grassmann who studied this issue and introduced the exterior product as a generalization of the cross product in 1844 [9]. The reason we cannot define the cross prod-

uct for arbitrary dimensions is that it relies on a vector perpendicular to the plane containing the two multiplying vectors, and for higher dimensions this vector is not unique. Instead, the exterior product encoded an oriented plane, which Grassmann called a bivector. The fact that the product was now intrinsic to the plane containing the pair of vectors made it possible to think of it in any dimensions, and for any number of vectors.

Although Grassmann’s work didn’t have a big impact at first, it ended up influencing the mathematician W. K. Clifford in his development of a geometric algebra. The exterior product was still not invertible, so motivated by Hamilton’s quaternion formulation, he combined inner and outer products into what he called the geometric product. The new product was not only invertible, but also defined a closed algebra. This is often referred to as Clifford algebra, although he originally referred to it as geometric algebra [10].

It is not until the second half of the 20th century that David Hestenes takes Clifford’s geometric algebra and constructs spacetime algebra (STA) from it, using Minkowski’s spacetime metric. This algebraic framework provides a unified approach for electromagnetism, classical mechanics and quantum mechanics, amongst other areas, which Hestenes himself develops in his work (see for instance [7, 11, 12]) drawing attention to the universal nature of the geometric algebra. Since then, many authors have continued developing spacetime algebra; in particular, it is worth mentioning Dressel, Bliokh and Nori’s comprehensive approach to the study of electromagnetism within the context of STA [13], and Doran and Lasenby’s work on the development of gauge theory gravity [14], along with their thorough introduction to geometric algebra and its applications in [15].

Spacetime algebra formulation of physics comes with a number of advantages, as will be seen in the following sections. Among other things, it allows a coordinate-free — and consequently reference-frame-independent — formulation, the unit imaginary I arises naturally from the geometry of spacetime, and many physical quantities are intrinsic to the framework, such as Pauli and Dirac matrices — they represent orthonormal bases in STA. These benefits provide a simple and straight-forward way of formulating many problems in physics, such as Maxwell’s equations of electromagnetism or the Kepler problem in classical mechanics, which makes spacetime algebra a remarkable tool for understanding physics.

In this chapter, we will first introduce the foundations of geometric algebra and build our way to spacetime algebra, revealing a number of properties that make the framework particularly advantageous. We will then be able to define the angular momentum bivector \mathbf{M} and derive a new expression for the gravitational force within the framework of STA.

2.1 Geometric algebra

The following four axioms govern the properties of the geometric product between vectors:

- (i) Associativity: $(ab)c = a(bc)$,
- (ii) Left-distributivity: $a(b + c) = ab + ac$,
- (iii) Right-distributivity: $(b + c)a = ba + ca$,

(iv) Contraction rule: $a^2 \in \mathbb{R}$.

Having defined its properties, from the geometric product ab one can define two new products, one that is symmetric,

$$a \cdot b = \frac{1}{2}(ab + ba) = b \cdot a, \quad (2.1)$$

and another one that is antisymmetric,

$$a \wedge b = \frac{1}{2}(ab - ba) = -b \wedge a. \quad (2.2)$$

Thus, the geometric product can be written as the sum of an inner (symmetric) and an outer (antisymmetric) product:

$$ab = a \cdot b + a \wedge b. \quad (2.3)$$

This is the canonical decomposition of the geometric product.

It is now interesting to see what the dot (\cdot) and the wedge (\wedge) products mean. On the one hand, from the contraction rule, we know that the inner product must be scalar-valued, and it can therefore be identified with the standard Euclidean dot product. On the other hand, the outer product describes an oriented plane segment, where commuting a and b changes the orientation of the plane. This is what Grassmann called a bivector. It can also be interpreted as the parallelogram obtained by sweeping one vector along the other (see Fig. 2.1). The magnitude of this outer product is the area of the parallelogram, $|a||b|\sin\theta$. It is this geometrical interpretation that makes it possible to generalize the wedge product to any dimensions, as opposed to the standard cross product.

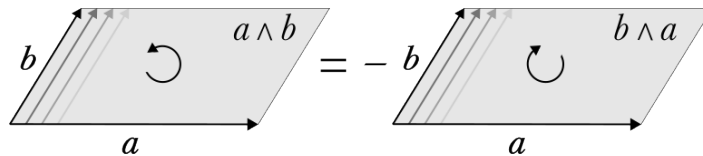


Figure 2.1: Bivectors $a \wedge b$ and $b \wedge a$, plane segments of opposite orientation, represented by parallelograms obtained by sweeping one vector along the other.

Let us discuss two important cases. We start from that of two orthogonal vectors. If two vectors a and b are orthogonal, we have $a \cdot b = 0$ and it follows from Eq. 2.1 that $ab = -ba$. Alternatively, two collinear vectors will define a parallelogram with vanishing area, which means $a \wedge b = 0$, and by Eq. 2.2 we will have $ab = ba$. We thus see that the geometric product provides a measure of the relative direction of two vectors. This will be more clear in Sect. 2.1.1. Therefore, commutativity means that the two vectors are collinear, while anticommutativity means orthogonality.

At this point we can start constructing the entire algebra, and we do this by successively multiplying vectors. In the same way that the geometric product of two vectors gives a scalar and a bivector, if we multiply a third vector c to a plane element $a \wedge b$ we will get a vector from

the inner product $(a \wedge b) \cdot c$ and an oriented volume from the outer product $(a \wedge b) \wedge c$. This volume is called a trivector, and is now symmetric, since the outer product is antisymmetric for vectors:

$$a \wedge b \wedge c = -a \wedge c \wedge b = c \wedge a \wedge b. \quad (2.4)$$

If we keep multiplying vectors, we will end up forming k -vectors, where k denotes the grade of the object. The geometric product of a vector v with a k -vector K can be generalized to

$$vK = v \cdot K + v \wedge K, \quad (2.5)$$

where the inner product generalizes to

$$v \cdot K = \frac{1}{2}(vK + (-1)^{k+1}Kv) = (-1)^{k+1}K \cdot v \quad (2.6)$$

and the corresponding outer product becomes

$$v \wedge K = \frac{1}{2}(vK - (-1)^kKv) = (-1)^kK \wedge v. \quad (2.7)$$

We therefore see that the symmetry of the inner and outer products alternate with the grade of the k -vector, as hinted by Eq. 2.4.

The important thing about Eq. 2.5 is that it decomposes vK in a $(k-1)$ -vector part and a $(k+1)$ -vector part. We thus say that the inner product *contracts* k -vectors and the outer product *inflates* them.

However, we have been able to see that vector multiplication does not generate pure k -vectors (unless the vectors are orthogonal, implying $a \cdot b = 0$). The way we deal with that is by introducing the concept of *multivector*. Multivectors are the elements of the n -dimensional geometric algebra \mathcal{G}_n , and combine objects of different grades. Consequently, the geometric product defines a closed algebra, and k -vectors form linearly independent subspaces of the total algebra.

Another advantage of defining the product as Eq. 2.3 is that although the dot and the wedge product are not invertible on their own, combining them into a single product retains enough information for the geometric product to be invertible, so we can define an inverse

$$a^{-1} = \frac{a}{a^2}. \quad (2.8)$$

We finally see that the geometric algebra thus defined overcomes the limitations that other products may encounter; the geometric product generates a closed and invertible algebra, and it therefore forms an appropriate algebraic framework to describe geometry.

Some of the interesting properties of geometric algebra may be seen by focusing on two and three dimensions.

2.1.1 Geometric algebra in two dimensions

All the elements in the two-dimensional geometric algebra \mathcal{G}_2 can be generated by the orthonormal set of vectors $\{\sigma_1, \sigma_2\}$, satisfying

$$\sigma_i \cdot \sigma_j = \delta_{ij}. \quad (2.9)$$

The only linearly independent elements we can generate from these basis vectors are 1 scalar, 2 vectors and 1 bivector:

$$\sigma_1^2 = \sigma_2^2 = 1 \quad ; \quad \{\sigma_1, \sigma_2\} \quad ; \quad \sigma_1 \sigma_2 = \sigma_1 \wedge \sigma_2. \quad (2.10)$$

The bivector $\sigma_1 \wedge \sigma_2$ is the highest grade element that can be generated in this algebra. It is not a coincidence that its grade corresponds to the dimension of the algebra; the outer product between this bivector and any of the other two basis vectors will be zero, which generalizes to geometric algebras of arbitrary dimension.

We call the highest grade element of a given algebra the *pseudoscalar*, and denote it by I . The reason behind the choice of this symbol is that it squares to -1 . In the two-dimensional case we are treating now,

$$I^2 = \sigma_1 \sigma_2 \sigma_1 \sigma_2 = -\sigma_1^2 \sigma_2^2 = -1. \quad (2.11)$$

Therefore, we have just found that the unit imaginary $I = \sqrt{-1}$ arises naturally from geometric considerations. Considering its properties in the plane happens to be very revealing. Let us first look into the effect of multiplying vectors by I :

$$\sigma_1 I = \sigma_1 \sigma_1 \sigma_2 = \sigma_2, \quad (2.12)$$

and

$$\sigma_2 I = \sigma_2 \sigma_1 \sigma_2 = -\sigma_2 \sigma_2 \sigma_1 = -\sigma_1. \quad (2.13)$$

Assuming that σ_1 and σ_2 form a right-handed pair, right-multiplication by I rotates vectors 90° anticlockwise (in a positive sense). Similarly, left-multiplication rotates 90° clockwise (in a negative sense).

In order to generalize rotations, we can instead consider the product between two arbitrary vectors a and b and try to get a dependence on the angle θ relating them. We can do that using the inner and outer products' geometric interpretations,

$$\begin{aligned} ab &= a \cdot b + a \wedge b = \\ &= |a||b| \cos \theta + |a||b| \sin \theta \sigma_1 \wedge \sigma_2 = |a||b|(\cos \theta + I \sin \theta) = |a||b|e^{I\theta}. \end{aligned} \quad (2.14)$$

Two important implications follow from this. On the one hand, the geometric product ab can be interpreted as a directed arc relating a and b in a circle of radius $|a||b|$. The factor $e^{I\theta}$ in Eq. 2.14 is called a *rotor*, and multiplying a and b by it gives

$$ae^{I\theta} = a \frac{ab}{|a||b|} = \frac{|a|}{|b|} b \quad (2.15)$$

and

$$e^{I\theta}b = \frac{ab}{|a||b|} b = \frac{|b|}{|a|} a, \quad (2.16)$$

so we can also say that the geometric product ab rotates and rescales a in order to get b , and vice versa. Consequently, multiplication of any vector by $e^{I\theta}$ generates a rotation in the plane I through an angle θ . This can be written as

$$x \rightarrow x' = xe^{I\theta}. \quad (2.17)$$

On the other hand, from Eq. 2.14 we find that the geometric product ab is a complex number of modulus $|a||b|$; its real and imaginary parts correspond to the inner and outer products, which reveals the geometric nature of the complex structure.

We have thus been able to understand some of the properties of geometric algebra by exploring it in two dimensions. The geometric algebra \mathcal{G}_2 is closely related to the algebra of complex numbers, and through this we have established a way to manipulate rotations in a simple and efficient way, without the need to introduce coordinates or matrices. Let us go a step further and see how this translates to three dimensions.

2.1.2 Geometric algebra in three dimensions

We will now consider the three-dimensional geometric algebra \mathcal{G}_3 , generated by the orthonormal basis $\{\sigma_1, \sigma_2, \sigma_3\}$. Multiplication between these vectors again satisfies Eq. 2.9.

The \mathcal{G}_3 algebra has four linearly independent subalgebras:

$$\sigma_1^2 = \sigma_2^2 = \sigma_3^2 = 1 \quad ; \quad \{\sigma_1, \sigma_2, \sigma_3\} \quad ; \quad \{\sigma_1\sigma_2, \sigma_2\sigma_3, \sigma_3\sigma_1\} \quad ; \quad \sigma_1\sigma_2\sigma_3, \quad (2.18)$$

so the complete algebra is spanned by 1 scalar, 3 vectors, 3 bivectors and 1 trivector.

The pseudoscalar is now the trivector $I = \sigma_1\sigma_2\sigma_3$, whose grade matches again the dimension of the algebra, and it follows that

$$I^2 = \sigma_1\sigma_2\sigma_3\sigma_1\sigma_2\sigma_3 = -\sigma_1\sigma_1\sigma_2\sigma_2\sigma_3\sigma_3 = -1, \quad (2.19)$$

using the anticommutativity of orthogonal vectors. Thus, we have found that a unit imaginary $I = \sqrt{-1}$ also appears naturally in three dimensions.

However, while in \mathcal{G}_2 multiplication by I caused a 90° rotation on vectors, the effect is different in the three-dimensional case. To see this, let us first examine $I\sigma_1$:

$$I\sigma_1 = \sigma_1\sigma_2\sigma_3\sigma_1 = \sigma_2\sigma_3, \quad (2.20)$$

so multiplication of a vector by I gives a bivector. Note that it is not necessary anymore to distinguish between left- and right-multiplication, since vectors in \mathcal{G}_3 commute with the pseudoscalar I .

We call multiplication by the pseudoscalar I a *duality* operation, since it transforms a vector in its dual bivector. In other words, every bivector in \mathcal{G}_3 can be written as the dual of a vector,

$$\mathbf{B} = Ib = bI, \quad (2.21)$$

where we represent bivectors in bold.

In fact, for the rest of the vectors in the generating set, we have

$$I\sigma_2 = \sigma_1\sigma_2\sigma_3\sigma_2 = \sigma_3\sigma_1 \quad (2.22)$$

and

$$I\sigma_3 = \sigma_1\sigma_2\sigma_3\sigma_3 = \sigma_1\sigma_2. \quad (2.23)$$

Thus, equations 2.20, 2.22 and 2.23 satisfy

$$\sigma_i \wedge \sigma_j = I\epsilon_{ijk}\sigma_k, \quad (2.24)$$

where ϵ_{ijk} is the completely antisymmetric Levi-Civita tensor.

A very interesting feature of geometric algebra arises if we extend this relation to include the complete geometric product,

$$\sigma_i\sigma_j = \sigma_i \cdot \sigma_j + \sigma_i \wedge \sigma_j = \delta_{ij} + I\epsilon_{ijk}\sigma_k. \quad (2.25)$$

This expression reminds us of the Pauli algebra of quantum mechanics. We can therefore say that Pauli matrices are a matrix representation of the orthonormal basis $\{\sigma_1, \sigma_2, \sigma_3\}$ of the geometric algebra \mathcal{G}_3 . The implications of this are remarkable; Pauli matrices are not inherently quantum mechanical but come instead with substantial geometric properties.

But let us focus anew on the vector-bivector duality. It leads to a particularly interesting equivalence, which we will find useful in the following sections. If we take Eq. 2.24 and identify $\epsilon_{ijk}\sigma_k$ as the result of the cross product $\sigma_i \times \sigma_j$, we can write

$$I\epsilon_{ijk}\sigma_k = I(\sigma_i \times \sigma_j) = \sigma_i \wedge \sigma_j, \quad (2.26)$$

which generalizes to any product as

$$Ia \times b = a \wedge b. \quad (2.27)$$

Thus, the standard cross product is dual to the outer product.

This result has significant consequences. The fact that we can translate from the three-dimensional standard algebra of Euclidean space to the geometric algebra \mathcal{G}_3 implies that we will be able to develop a three-dimensional geometric calculus, allowing us to manipulate physical quantities such as those from classical mechanics in the framework of geometric algebra.

After introducing the concept of duality, we can now write multivectors in \mathcal{G}_3 in their extended form as

$$M = \alpha + a + Ib + I\beta, \quad (2.28)$$

where α and β represent scalars and a and b represent vectors.

From this, one can also notice that trivectors are dual to scalars, and in the two-dimensional case we dealt with in the last section, it was bivectors that were dual to scalars. This is in fact why we use the *pseudo* prefix together with *scalar* to denote the highest grade element; because it is always the scalars dual.

Rotations

In a similar manner to how the two-dimensional geometric algebra provided an easy way of handling rotations, \mathcal{G}_3 formulation allows a simple and coordinate-free treatment of rotations and reflections in space. Reflections will not be addressed in this report, suffice it to say that they work in a similar way to rotations (see [7] for a proper description).

We already defined a rotor in the previous section, and saw how it transforms vectors in Eq. 2.17. In three-dimensions, this transformation generalizes to

$$x \rightarrow x' = Rx\tilde{R} = e^{-\mathbf{B}\theta/2}xe^{\mathbf{B}\theta/2}, \quad (2.29)$$

where R denotes a rotor and \tilde{R} is its *reverse*, and the two-sided multiplication by it generates a rotation through an angle θ in the plane described by the bivector \mathbf{B} .

This is a good point to pause and introduce the reversion operator. Under this transformation, the order of all geometric products is reversed, in such a way that a bivector's reverse is its negation $\tilde{\mathbf{B}} = (a \wedge b)^\sim = b \wedge a = -\mathbf{B}$ and thus the rotor $R = e^{-\mathbf{B}\theta/2}$ becomes

$$\tilde{R} = (e^{-\mathbf{B}\theta/2})^\sim = \cos(\theta/2) - \tilde{\mathbf{B}} \sin(\theta/2) = e^{\mathbf{B}\theta/2}. \quad (2.30)$$

There are two things to note on how we generalized Eq. 2.17 into Eq. 2.29. The first is that while $I = \sigma_1\sigma_2$ was the only plane of rotation in \mathcal{G}_2 , we now have three linearly independent bivectors in the algebra and the number of planes we can rotate a vector in is thus infinite. Hence, we need to specify the plane by the bivector \mathbf{B} .

The second noticeable thing is that we are now multiplying the rotor on both sides and using the half-angle $\theta/2$, instead of using θ and multiplying on just one side. The reason behind this is that when rotating a vector, it is only its component in the plane that is affected, as seen in Fig. 2.2, and the two-sided multiplication allows this by choosing this component. To see this, we can decompose the vector x into its component orthogonal to the plane, x_\perp , and its component in the plane, x_\parallel . The rotated vector x' is given by

$$x' = Rx\tilde{R} = Rx_\perp\tilde{R} + Rx_\parallel\tilde{R} = R\tilde{R}x_\perp + RRx_\parallel = x_\perp + R^2x_\parallel, \quad (2.31)$$

where we have used that x_\perp commutes with the bivector \mathbf{B} , and thus with \tilde{R} , and x_\parallel anti-commutes with them.

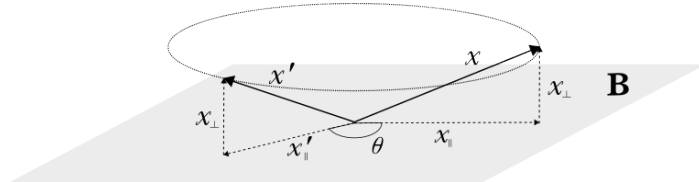


Figure 2.2: Rotation of a vector x into the transformed vector x' in the plane \mathbf{B} through an angle θ . The figure shows how it is only the component in the plane that is rotated, while the orthogonal component is left intact.

We therefore see that by multiplying both the rotor and its conjugate on each side of the vector, the squared rotor only affects the component x_{\parallel} ; as a consequence, we recover our expression from Eq. 2.17 and the rotation ends up being through an angle θ .

It is due to the simple treatment of rotations provided by Eq. 2.29 that the geometric algebra of space becomes such a powerful tool for solving problems in classical mechanics, i.e. rigid body physics or the two-body problem. A detailed description of these applications can be found in Hestenes' book *New Foundations for Classical Mechanics* [16] and, in particular, T. Vold's approach to geometric algebra's application in rigid body mechanics [17] is specially instructive.

Now that we have introduced geometric algebra and seen its implications in two and three dimensions, which has served to gain a better understanding of the framework by example, we are ready to extend the formulation to Minkowski spacetime and introduce the so called *spacetime algebra*.

2.2 Spacetime algebra

Up to this point we have been constructing our algebras by choosing a set of orthonormal vectors that satisfied Eq. 2.9 as a generating basis. In order to define the geometric algebra of spacetime $\mathcal{G}_4 = \mathcal{G}(\mathcal{M}^4)$, the standard frame $\{\gamma_{\mu}\}_{\mu=0}^3$ must instead satisfy

$$\gamma_{\mu} \cdot \gamma_{\nu} = \eta_{\mu\nu}, \quad (2.32)$$

where $\eta_{\mu\nu}$ is the Minkowski metric of signature $(+, -, -, -)$.

By iteratively multiplying γ_{μ} we can form five linearly independent subalgebras

$$1, \quad \{\gamma_{\mu}\}, \quad \{\gamma_{\mu}\gamma_{\nu}\}, \quad \{\gamma_{\mu}\gamma_{\nu}\gamma_{\rho}\}, \quad \gamma_0\gamma_1\gamma_2\gamma_3, \quad (2.33)$$

generated by 1 scalar, 4 vectors, 6 bivectors, 4 trivectors and a 4-vector¹, respectively:

$$1, \quad \{\gamma_0, \gamma_1, \gamma_2, \gamma_3\}, \quad \{\gamma_{10}, \gamma_{20}, \gamma_{30}, \gamma_{12}, \gamma_{23}, \gamma_{31}\}, \quad \{\gamma_{123}, \gamma_{023}, \gamma_{310}, \gamma_{012}\}, \quad \gamma_{0123}. \quad (2.34)$$

Since we are dealing with spacetime, it is useful to distinguish between *timelike*, *spacelike* and *lightlike* elements. The sorting is made in relation to their *signature* ϵ . When we defined the geometric product at the very beginning of this chapter, the contraction rule that was the fourth axiom dictated that $a^2 \in \mathbb{R}$ for a vector a . In terms of a signature, we can rewrite that as

$$a^2 = \epsilon|a|^2, \quad (2.35)$$

and thus we say the vector is timelike if $\epsilon = 1$, spacelike if $\epsilon = -1$ or lightlike if $|a| = 0$. In the standard frame $\{\gamma_{\mu}\}$, for example, we have the timelike vector γ_0 and the spacelike vectors γ_i with $i = 1, 2, 3$. This distinction extends to any element of the algebra; it is easy to see that in the case of bivectors γ_{10}, γ_{20} and γ_{30} are timelike, while γ_{12}, γ_{23} and γ_{31} are

¹Here and in the following, 4-vector refers to a k -vector of grade $k = 4$, as opposed to four-vectors from special relativity. The latter are actually 1-vectors in a geometric algebra of four dimensions.

spacelike.

The pseudoscalar of this algebra is the 4-vector γ_{0123} . In fact,

$$\begin{aligned} I^2 &= \gamma_0\gamma_1\gamma_2\gamma_3\gamma_0\gamma_1\gamma_2\gamma_3 = -\gamma_0\gamma_1\gamma_2\gamma_0\gamma_1\gamma_2\gamma_3\gamma_3 = \\ &= -\gamma_0\gamma_1\gamma_0\gamma_1\gamma_2\gamma_2\gamma_3\gamma_3 = \gamma_0\gamma_0\gamma_1\gamma_1\gamma_2\gamma_2\gamma_3\gamma_3 = -1, \end{aligned} \quad (2.36)$$

where we used that orthogonal vectors anticommute, as well as $\gamma_0^2 = 1$ and $\gamma_i^2 = -1$ for $i = 1, 2, 3$. Thus, we once more find a unit imaginary I from the geometric structure, spacetime in this case.

Let us now consider the different dualities. We start by finding the dual of a vector, by computing $\gamma_0 I$:

$$\gamma_0 I = \gamma_0\gamma_0\gamma_1\gamma_2\gamma_3 = \gamma_1\gamma_2\gamma_3 = \gamma_{123}. \quad (2.37)$$

Similarly, we will have

$$\gamma_1 I = \gamma_1\gamma_0\gamma_1\gamma_2\gamma_3 = \gamma_0\gamma_2\gamma_3 = \gamma_{023}, \quad (2.38)$$

$$\gamma_2 I = \gamma_2\gamma_0\gamma_1\gamma_2\gamma_3 = -\gamma_0\gamma_1\gamma_3 = -\gamma_{013} = \gamma_{310}, \quad (2.39)$$

$$\gamma_3 I = \gamma_3\gamma_0\gamma_1\gamma_2\gamma_3 = \gamma_0\gamma_1\gamma_2 = \gamma_{012}. \quad (2.40)$$

We see that the vector subalgebra's dual is the trivector subalgebra, and thus we can call trivectors pseudovectors.

It is important to note that vectors anticommute with the pseudoscalar I , as opposed to the three-dimensional case. In fact, it is easy to verify from equations 2.37 – 2.40 that left-multiplication of vectors $\{\gamma_\mu\}_{\mu=0}^3$ by I will lead to trivectors of opposite sign. This means that since any vector a can be written as a linear combination of $\{\gamma_\mu\}_{\mu=0}^3$ in the form $a = a_0\gamma_0 + a_1\gamma_1 + a_2\gamma_2 + a_3\gamma_3$, it will anticommute with I .

So far we have seen that in the \mathcal{G}_4 algebra of spacetime scalars' duals are 4-vectors (pseudoscalars) and vectors' duals are trivectors (pseudovectors). We can additionally take a look at how bivectors change under a duality transformation. To do this, let us examine the product $\gamma_{10} I$

$$\gamma_{10} I = \gamma_1\gamma_0\gamma_0\gamma_1\gamma_2\gamma_3 = -\gamma_2\gamma_3 = -\gamma_{23}. \quad (2.41)$$

Therefore, from multiplying a bivector by I we get another bivector orthogonal to it. If we check the rest of the elements in the bivector subalgebra $\{\gamma_\mu\gamma_\nu\}$, we can see that bivectors are their own duals. Their duality relations can be summarized by

$$\gamma_{i0} I = -\epsilon_{ijk}\gamma_{jk} \quad (2.42)$$

and

$$\gamma_{jk} I = \epsilon_{ijk}\gamma_{i0}. \quad (2.43)$$

We thus say that bivectors define a *self-dual* subalgebra.

In contrast with how vectors anticommute with I , bivectors commute with it, which can be easily checked from Eq. 2.41. Consequently, we can say that I commutes with even-graded

subalgebras (scalars, bivectors) and anticommutes with odd-graded subalgebras (vectors).

Taking all dualities into account, we can express multivectors $M \in \mathcal{G}(\mathcal{M}^4)$ as

$$M = \alpha + a + \mathbf{B} + bI + \beta I = \alpha + a + \mathbf{B} - Ib + I\beta, \quad (2.44)$$

where we see that they consist of a complex scalar $\lambda = \alpha + \beta I$, a complex vector $c = a + bI$ and a bivector \mathbf{B} .

Before proceeding further into rotations in spacetime, it is worth noting the reason behind the particular choice of the symbol representing the basis vectors $\{\gamma_\mu\}_{\mu=0}^3$. Taking Eq. 2.32, we can extend it and get to

$$\gamma_\mu \gamma_\nu + \gamma_\nu \gamma_\mu = 2\eta_{\mu\nu}, \quad (2.45)$$

which is the anticommutation relation defining the Dirac matrix algebra. Consequently, the Dirac matrices define a representation of the algebra of spacetime $\mathcal{G}(\mathcal{M}^4)$, which means their connection to relativistic quantum mechanics is not intrinsic, as for the case of the Pauli matrices; they instead characterize spacetime geometry.

2.2.1 Lorentz transformations

When we discussed the geometric algebras of two and three dimensions we obtained a simple formulation for rotations. Using rotors of the form $R = e^{-\mathbf{B}\theta/2}$, we could rotate vectors by an angle θ in a plane defined by the bivector \mathbf{B} . An important advantage of this formulation is that it is generalizable to geometric algebras of any dimension, and this includes spacetime algebra.

In fact, the bivector basis $\{\gamma_{\mu\nu}\}$ forms the Lie algebra of the Lorentz group, and as a consequence Eq. 2.29 generates Lorentz transformations in $\mathcal{G}(\mathcal{M}^4)$. In order to see this, we define a commutator bracket for bivectors that will give us the relations defining the generators of the Lorentz group [13].

We begin by considering the product of two bivectors \mathbf{A} and \mathbf{B} . It turns out that the antisymmetric part of \mathbf{AB} , that we write as a commutator bracket,

$$[\mathbf{A}, \mathbf{B}] \equiv \frac{1}{2}(\mathbf{AB} - \mathbf{BA}), \quad (2.46)$$

gives a third bivector. To see that, let us compute the commutator relations between the six bivectors that constitute the basis. For the spacelike bivectors γ_{12}, γ_{23} and γ_{31} we get the following relations

$$[\gamma_{12}, \gamma_{23}] = \gamma_{31} \quad [\gamma_{23}, \gamma_{31}] = \gamma_{12} \quad [\gamma_{31}, \gamma_{12}] = \gamma_{23} \quad . \quad (2.47)$$

For the timelike bivectors, we get

$$[\gamma_{10}, \gamma_{20}] = -\gamma_{12} \quad [\gamma_{20}, \gamma_{30}] = -\gamma_{23} \quad [\gamma_{30}, \gamma_{10}] = -\gamma_{31}. \quad (2.48)$$

And if we mix spacelike and timelike bivectors we get the rest of the commutation relations

$$\begin{aligned}
[\gamma_{12}, \gamma_{10}] &= \gamma_{20}, & [\gamma_{23}, \gamma_{20}] &= \gamma_{30}, & [\gamma_{31}, \gamma_{30}] &= \gamma_{10}, \\
[\gamma_{31}, \gamma_{10}] &= -\gamma_{30}, & [\gamma_{12}, \gamma_{20}] &= -\gamma_{10}, & [\gamma_{23}, \gamma_{30}] &= -\gamma_{20}, \\
[\gamma_{23}, \gamma_{10}] &= 0, & [\gamma_{31}, \gamma_{20}] &= 0, & [\gamma_{12}, \gamma_{30}] &= 0.
\end{aligned} \tag{2.49}$$

We can now denote our bivectors by $\mathbf{S}_1 = \gamma_{23}$, $\mathbf{S}_2 = \gamma_{31}$, $\mathbf{S}_3 = \gamma_{12}$ and $\mathbf{K}_1 = \gamma_{10}$, $\mathbf{K}_2 = \gamma_{20}$, $\mathbf{K}_3 = \gamma_{30}$ and summarize the commutation relations in Eq. 2.47, 2.48 and 2.49 respectively as

$$[\mathbf{S}_i, \mathbf{S}_j] = \epsilon_{ijk} \mathbf{S}_k, \quad [\mathbf{K}_i, \mathbf{K}_j] = -\epsilon_{ijk} \mathbf{S}_k, \quad [\mathbf{S}_i, \mathbf{K}_j] = \epsilon_{ijk} \mathbf{K}_k. \tag{2.50}$$

Thus, bivectors in $\mathcal{G}(\mathcal{M}^4)$ form the closed nonassociative Lie algebra of the restricted Lorentz group. In particular, the spacelike bivectors \mathbf{S}_i generate rotations in space and timelike bivectors \mathbf{K}_i generate boosts.

It follows from this that we can find the Lorentz transform M' of a multivector M through Eq. 2.29 by choosing the plane of rotation to be any of the generators of the Lorentz group. Thus, spacetime algebra reduces Lorentz transformations to simple rotor multiplication, enabling once more an easy and coordinate-free formulation.

2.2.2 Spacetime split

One of the main advantages of STA is that we can formulate conventional relativistic physics without the need to refer to a coordinate system. However, it is sometimes useful to write equations in terms of variables tied to a specific inertial system, which brings us to the concept of *spacetime split*.

We can characterize a given inertial system by the timelike unit vector γ_0 [11]. By choosing this particular reference frame, we can connect the spacetime algebra of $\mathcal{G}(\mathcal{M}^4)$ to its even subalgebra $\mathcal{G}_3 = \mathcal{G}(\mathcal{P}^3)$, where $\mathcal{P}^3 = \mathcal{P}^3(\gamma_0)$ consists of all bivectors generated by the set $\{\gamma_{10}, \gamma_{20}, \gamma_{30}\}$. We can decompose these bivectors as

$$\vec{\sigma}_i \equiv \gamma_{i0} = \gamma_i \wedge \gamma_0. \tag{2.51}$$

If we now take the standard basis $\{\vec{\sigma}_i; i = 1, 2, 3\}$ introduced in Sect. 2.1.2 for \mathcal{P}^3 , \mathcal{P}^3 will be the Pauli algebra embedded within $\mathcal{G}(\mathcal{M}^4)$.

The elements $\vec{\sigma}_i$ correspond to the three spatial directions γ_i orthogonal to γ_0 , and thus generate the vector quantities with three spatial components that we use in standard vector analysis. These vectors are called *relative vectors* because they are relative to the γ_0 -system, and we use arrows to distinguish them from vectors in $\mathcal{G}(\mathcal{M}^4)$.

In order to understand spacetime split and how choosing a reference frame γ_0 leads to it, let us consider the example of the position vector x . We can write it in terms of the generating vectors as $x = ct\gamma_0 + x_1\gamma_1 + x_2\gamma_2 + x_3\gamma_3$. Multiplying x by γ_0 yields

$$x\gamma_0 = x \cdot \gamma_0 + x \wedge \gamma_0 = ct + x_1\vec{\sigma}_1 + x_2\vec{\sigma}_2 + x_3\vec{\sigma}_3 = ct + \vec{x}. \tag{2.52}$$

Thus, spacetime split separates vectors into a relative scalar and a relative vector. We call this combination a *paravector*.

The reverse of Eq. 2.52 is

$$(x\gamma_0)^\sim = \gamma_0 x = \gamma_0 \cdot x + \gamma_0 \wedge x = ct - \vec{x}. \quad (2.53)$$

Hence, combining Eqs. 2.52 and 2.53 we get the interval

$$x^2 = x\gamma_0\gamma_0x = (ct + \vec{x})(ct - \vec{x}) = (ct)^2 - |\vec{x}|^2. \quad (2.54)$$

We can see that the interval between two events does not depend on the chosen inertial frame and it is thus Lorentz invariant.

It is interesting to further explore some important physical quantities and their spacetime splits. Let us examine the proper velocity $v = dx/d\tau$:

$$v\gamma_0 = \frac{dx}{d\tau} \cdot \gamma_0 + \frac{dx}{d\tau} \wedge \gamma_0 = c \frac{dt}{d\tau} + \frac{d\vec{x}}{d\tau} = c \frac{dt}{d\tau} + \frac{d\vec{x}}{dt} \frac{dt}{d\tau} = \frac{dt}{d\tau} (c + \vec{v}), \quad (2.55)$$

where $\vec{v} = d\vec{x}/dt$ is the *relative velocity* and $\frac{dt}{d\tau}$ is the Lorentz or *time dilation* factor denoted by γ .

The value of the Lorentz factor γ can be obtained from

$$v^2 = v\gamma_0\gamma_0v = \frac{dt}{d\tau} (c + \vec{v}) \frac{dt}{d\tau} (c - \vec{v}) = \left(\frac{dt}{d\tau} \right)^2 (c^2 - |\vec{v}|^2). \quad (2.56)$$

Noting that $v^2 = c^2$,

$$\left(\frac{dt}{d\tau} \right)^2 (c^2 - |\vec{v}|^2) = c^2 \Rightarrow \gamma = \frac{dt}{d\tau} = \sqrt{\frac{c^2}{c^2 - |\vec{v}|^2}} = \frac{1}{\sqrt{1 - \frac{|\vec{v}|^2}{c^2}}}. \quad (2.57)$$

The spacetime split of the proper momentum p into the energy E and the relative momentum \vec{p} is

$$p\gamma_0 = \frac{E}{c} + \vec{p}. \quad (2.58)$$

Squaring p gives the invariant quantity

$$p^2 = \left(\frac{E}{c} + \vec{p} \right) \left(\frac{E}{c} - \vec{p} \right) = \left(\frac{E}{c} \right)^2 - |\vec{p}|^2, \quad (2.59)$$

and we can thus relate it to the proper mass $m^2c^2 = (E/c)^2 - |\vec{p}|^2$.

It therefore follows that the proper momentum – or energy-momentum vector – is conserved, which makes this formulation advantageous once more. While we were able to see this by merely considering spacetime geometry, deriving energy-momentum conservation using standard vector analysis requires a longer derivation, as can be seen in Appendix A.

Another interesting quantity is the electromagnetic field bivector \mathbf{F} , that splits into electric and magnetic parts. However, instead of needing to distinguish between polar and axial vectors, the distinction here has a truly geometrical meaning; \vec{E} is a relative vector and $I\vec{B}$ is a relative bivector. We can write the electromagnetic field \mathbf{F} in terms of the bivector basis as

$$\begin{aligned}\mathbf{F} &= E_1\gamma_{10} + E_2\gamma_{20} + E_3\gamma_{30} + B_1\gamma_{32} + B_2\gamma_{13} + B_3\gamma_{21} = \\ &= E_1\gamma_{10} + E_2\gamma_{20} + E_3\gamma_{30} + B_1\gamma_{10}I + B_2\gamma_{20}I + B_3\gamma_{30}I,\end{aligned}\tag{2.60}$$

following the bivector dualities from Eq. 2.42. From definition 2.51, its spacetime split gives

$$\mathbf{F} = E_1\vec{\sigma}_1 + E_2\vec{\sigma}_2 + E_3\vec{\sigma}_3 + B_1\vec{\sigma}_1I + B_2\vec{\sigma}_2I + B_3\vec{\sigma}_3I = \vec{E} + \vec{B}I.\tag{2.61}$$

It is worth noting that this time we have been able to split \mathbf{F} into a relative vector and a relative bivector without the need to multiply it by a specific inertial system γ_0 ; since \mathbf{F} is a bivector, it is sufficient to write it in terms of the relative basis $\{\vec{\sigma}_i\}$.

The quantity we are interested in in this work is the angular momentum bivector \mathbf{M} , which has a relative form similar to that of the electromagnetic field bivector \mathbf{F} . This will be dealt with in the following section.

2.3 Derivation of the gravitational force

After having introduced the spacetime algebra $\mathcal{G}(\mathcal{M}^4)$ and its properties, we are now ready to derive a gravitational force.

As suggested in [6], we start by defining the angular momentum bivector \mathbf{M} as a generalization of the three-dimensional angular momentum:

$$\mathbf{M} = x \wedge p,\tag{2.62}$$

where x is the proper position and p is the proper momentum. Their spacetime splits are given by Eqs. 2.52 and 2.58, and we can rewrite them as $x = \gamma_0(ct - \vec{x})$ and $p = (E/c + \vec{p})\gamma_0$. Using these expressions, Eq. 2.62 yields

$$\begin{aligned}\mathbf{M} &= \gamma_0(ct - \vec{x}) \wedge \left(\frac{E}{c} + \vec{p}\right)\gamma_0 = \\ &= \gamma_0\left(ct \wedge \frac{E}{c}\right)\gamma_0 - \gamma_0\left(\vec{x} \wedge \frac{E}{c}\right)\gamma_0 + \gamma_0(ct \wedge \vec{p})\gamma_0 - \gamma_0(\vec{x} \wedge \vec{p})\gamma_0.\end{aligned}\tag{2.63}$$

The first term in Eq. 2.63 is the wedge product of two scalars, which gives 0. Since γ_0 anticommutes with relative vectors, and using the duality in Eq. 2.27, the angular momentum bivector \mathbf{M} becomes

$$\mathbf{M} = \frac{E}{c}\vec{x} - ct\vec{p} - \vec{x} \times \vec{p}I.\tag{2.64}$$

It is now possible to identify the dynamic mass moment $\vec{N} = ct\vec{p} - E\vec{x}/c$ as given by [18] and the angular momentum $\vec{L} = \vec{x} \times \vec{p}$. Eq. 2.64 hence takes the final form

$$\mathbf{M} = -c\vec{N} - \vec{L}I.\tag{2.65}$$

We thus see that similarly to how the bivector \mathbf{F} combines the electric \vec{E} and magnetic \vec{B} fields, \mathbf{M} combines the dynamic mass moment \vec{N} and the angular momentum \vec{L} .

Now that the angular momentum bivector is defined we can proceed with the derivation of the gravitational force, which is given by the contraction of \mathbf{M} with mv , where m is the mass of the particle and v is its proper velocity.

The fact that the force takes this form can be demonstrated as follows [15, 19]. Consider a particle of mass m on a trajectory $x(\tau)$, with the velocity given by $v(\tau) = \dot{x}$. At a later time, the proper velocity will be given by

$$v(\tau + \Delta\tau) = Rv(\tau)\tilde{R}. \quad (2.66)$$

This transformation, that we recognize from Eq. 2.29, is a pure Lorentz boost generated by the set of timelike bivectors $\{\gamma_{i0}\}$ contained inside the rotor $R = R(\tau)$. Our rotor will therefore have the usual form

$$R = e^{-\mathbf{B}\Delta\tau/2}, \quad (2.67)$$

where the bivector \mathbf{B} contains the boost generators. We do not need to look too far in order to find such a bivector; it turns out that the angular momentum bivector we defined in Eq. 2.65 is written in terms of the relative basis $\{\vec{\sigma}_i \equiv \gamma_{i0}\}$, so it will indeed be a boost generator. Therefore, the rotor R will be given by

$$R = e^{-\mathbf{M}\Delta\tau/2} = e^{(c\vec{N} + \vec{L}I)\Delta\tau/2}. \quad (2.68)$$

We can now examine the proper acceleration \dot{v} ,

$$\dot{v}(\tau + \Delta\tau) = \dot{R}v(\tau)\tilde{R} + Rv(\tau)\dot{\tilde{R}}. \quad (2.69)$$

It follows from Eq. 2.66 that

$$\tilde{R}v(\tau + \Delta\tau) = v(\tau)\tilde{R} \quad (2.70)$$

and

$$v(\tau + \Delta\tau)R = Rv(\tau). \quad (2.71)$$

Inserting Eqs. 2.70 and 2.71 into 2.69 yields

$$\dot{v}(\tau + \Delta\tau) = \dot{R}\tilde{R}v(\tau + \Delta\tau) + v(\tau + \Delta\tau)R\dot{\tilde{R}}, \quad (2.72)$$

which we can further simplify by noting that $(\dot{R}\tilde{R})^\sim = R\dot{\tilde{R}} = -\dot{R}\tilde{R}$, because $\dot{R}\tilde{R}$ defines a bivector and therefore its reverse is its own negation, as we mentioned earlier. Thus, the acceleration becomes

$$\dot{v}(\tau + \Delta\tau) = \dot{R}\tilde{R}v(\tau + \Delta\tau) - v(\tau + \Delta\tau)\dot{R}\tilde{R} = 2\dot{R}\tilde{R} \cdot v(\tau + \Delta\tau). \quad (2.73)$$

Note that the dot product of a bivector with a vector is antisymmetric (recall 2.6).

If we compute the bivector $2\dot{R}\tilde{R}$ using $R = e^{-\mathbf{M}\Delta\tau/2}$,

$$2\dot{R}\tilde{R} = -\mathbf{M}e^{-\mathbf{M}\Delta\tau/2}e^{\mathbf{M}\Delta\tau/2} = -\mathbf{M}, \quad (2.74)$$

we finally get to the equation of motion

$$\dot{v} = -\mathbf{M} \cdot v. \quad (2.75)$$

This is the acceleration of the particle, caused by the angular momentum bivector \mathbf{M} . Of course, had we used a different bivector in Eq. 2.68, the acceleration would have been due to said bivector. One gets the equivalent result, for example, when applying the electromagnetic field bivector \mathbf{F} .

If we now insert the mass of the particle in Eq. 3.7, we get the gravitational force

$$m\dot{v} = -m\mathbf{M} \cdot v. \quad (2.76)$$

Thus, we just saw that we can derive a gravitational force by contracting the angular momentum bivector \mathbf{M} with the proper velocity v and multiplying it by the mass of the particle.

Let us compute Eq. 3.7, using the definition of the angular momentum bivector from Eq. 2.65 and the spacetime split of the proper velocity, $v = (c\gamma + \vec{v}\gamma)\gamma_0$, computed in Eq. 2.55.

$$\begin{aligned} \dot{v} &= -\mathbf{M} \cdot v = \frac{1}{2}((- \mathbf{M})v - v(- \mathbf{M})) = \\ &= \frac{1}{2} \left[(c\vec{N} + \vec{L}I)(c\gamma + \vec{v}\gamma)\gamma_0 - (c\gamma + \vec{v}\gamma)\gamma_0(c\vec{N} + \vec{L}I) \right] = \\ &= \frac{1}{2} \left[(c\vec{N} + \vec{L}I)(c\gamma + \vec{v}\gamma)\gamma_0 + (c\gamma + \vec{v}\gamma)(c\vec{N} - \vec{L}I)\gamma_0 \right], \end{aligned} \quad (2.77)$$

where we used that γ_0 anticommutes with \vec{N} and commutes with $\vec{L}I$ ². If we expand the products and reorganize the terms,

$$\begin{aligned} \dot{v} &= \frac{1}{2} \left[c^2\vec{N} + c\vec{L}I + c\vec{N}\vec{v} + \vec{L}I\vec{v} + c^2\vec{N} - c\vec{L}I + c\vec{v}\vec{N} - \vec{v}\vec{L}I \right] \gamma\gamma_0 = \\ &= \left[c^2\vec{N} + c\frac{1}{2}(\vec{N}\vec{v} + \vec{v}\vec{N}) + \frac{1}{2}(\vec{L}I\vec{v} - \vec{v}\vec{L}I) \right] \gamma\gamma_0 = \left(c^2\vec{N} + c\vec{N} \cdot \vec{v} - \vec{v} \wedge \vec{L}I \right) \gamma\gamma_0, \end{aligned} \quad (2.78)$$

and if we use the duality $\vec{v} \wedge \vec{L}I = -\vec{v} \times \vec{L}$ given by 2.27, we get to the final result

$$\dot{v} = (c\vec{N} \cdot \vec{v})\gamma\gamma_0 + (c^2\vec{N} + \vec{v} \times \vec{L})\gamma\gamma_0. \quad (2.79)$$

Finally, inserting the mass m and taking γ_0 to the left-hand side yields the gravitational force

$$m\dot{v}\gamma_0 = mc\gamma\vec{N} \cdot \vec{v} + m\gamma(c^2\vec{N} + \vec{v} \times \vec{L}). \quad (2.80)$$

Note that this is a *proper* gravitational force; we are looking at its spacetime split.

It is the vector part on the right-hand side of the equation that we are interested in. It represents the gravitational force $md\vec{v}/dt$ in the relative frame γ_0 – and the scalar part can be interpreted as its corresponding rate of work. As we can see, it has two terms: one

²This is because γ_0 anticommutes with any timelike bivector γ_{i0} , which is the basis of \vec{N} and \vec{L} . However, when having $\vec{L}I$, the basis is the dual set of bivectors $\{\gamma_{ij}\}$, and γ_0 commutes with those.

proportional to \vec{N} and the other proportional to $\vec{v} \times \vec{L}$. We will show in Sect. 2.3.1 that the \vec{N} term is nothing more than the usual Newtonian force, so it is the $\vec{v} \times \vec{L}$ term that distinguishes the force derived within STA from the standard gravitational force.

The resemblance between Eq. 2.80 and the Lorentz force $q(c\vec{E} + \vec{v} \times \vec{B})$ is evident. In fact, the Lorentz force can be derived from contracting the field bivector $\mathbf{F} = \vec{E} + \vec{B}I$ with a charge current qv , in a completely analogous way to how we derived the gravitational force (see [13]).

2.3.1 Computation of \vec{N} and \vec{L}

Before moving forward to the numerical implementation of the force in Eq. 2.80, we will need to obtain expressions for \vec{N} and \vec{L} so that we can understand what they mean. In order to do that, we will start by finding the equivalent version of Maxwell's equations of electromagnetism for the gravitational case.

The electromagnetic theory is discussed by Dressel, Bliokh and Nori in [13]. Besides deriving the Lorentz force, they show that within STA, Maxwell's equations with sources are reduced to the single equation $\nabla \mathbf{F} = j_{\mathbf{F}}$, with the source $j_{\mathbf{F}}$ consisting of an electric source vector j_e and a magnetic source trivector $j_m I$. As we can see from comparing Eqs. 2.61 and 2.65, the gravitational case should be completely analogous. We can therefore describe the evolution of the angular momentum bivector \mathbf{M} as

$$\nabla \mathbf{M} = j_{\mathbf{M}}. \quad (2.81)$$

Let us expand Eq. 2.81. Since $\nabla \mathbf{M} = \nabla \cdot \mathbf{M} + \nabla \wedge \mathbf{M}$, it will give a vector and a trivector part. We can compute this by using the spacetime split of the vector derivative, $\nabla = \gamma_0(\partial_0 + \vec{\nabla})$:

$$\begin{aligned} \nabla \mathbf{M} &= \gamma_0(\partial_0 + \vec{\nabla})(-c\vec{N} - \vec{L}I) = \gamma_0 \left[-c\partial_0\vec{N} - \partial_0\vec{L}I - c\vec{\nabla}\vec{N} - \vec{\nabla}\vec{L}I \right] = \\ &= \gamma_0 \left[-c\partial_0\vec{N} - \partial_0\vec{L}I - c\vec{\nabla} \cdot \vec{N} - c\vec{\nabla} \wedge \vec{N} - \vec{\nabla} \cdot \vec{L}I - \vec{\nabla} \wedge \vec{L}I \right] \\ &= \gamma_0 \left[-c\partial_0\vec{N} - c\vec{\nabla} \cdot \vec{N} + \vec{\nabla} \times \vec{L} \right] + \gamma_0 \left[-\partial_0\vec{L} - \vec{\nabla} \cdot \vec{L} - c\vec{\nabla} \times \vec{N} \right] I, \end{aligned} \quad (2.82)$$

where we used that $\vec{\nabla} \wedge \vec{N} = \vec{\nabla} \times \vec{N}I$ and $\vec{\nabla} \wedge \vec{L}I = -\vec{\nabla} \times \vec{L}I$.

Now that we can explicitly see the vector and trivector parts, we can write the source as $j_{\mathbf{M}} = j_1 + j_3I$, being j_1 and j_3 both vectors. Thus, Eq. 2.82 can be split into

$$\begin{aligned} \gamma_0 \left[-c\partial_0\vec{N} - c\vec{\nabla} \cdot \vec{N} + \vec{\nabla} \times \vec{L} \right] &= j_1, \\ \gamma_0 \left[-\partial_0\vec{L} - \vec{\nabla} \cdot \vec{L} - c\vec{\nabla} \times \vec{N} \right] &= j_3. \end{aligned} \quad (2.83)$$

At the same time, each of these equations has a scalar and a vectorial part, so by spacetime

splitting the sources as $j_i = \gamma_0(c\rho_i - \vec{J}_i)$ we get the four equations:

$$\begin{aligned}
\vec{\nabla} \cdot \vec{N} &= -\rho_1, \\
\vec{\nabla} \cdot \vec{L} &= -c\rho_3, \\
c\partial_0\vec{N} - \vec{\nabla} \times \vec{L} &= \vec{J}_1, \\
\partial_0\vec{L} + c\vec{\nabla} \times \vec{N} &= \vec{J}_3.
\end{aligned} \tag{2.84}$$

This is the gravitational version of Maxwell's equations of electromagnetism, which describe the evolution of \vec{N} and \vec{L} . In order to solve these equations, we will need to define the sources.

On the one hand, there is j_1 . From its spacetime split, we see that its scalar part will generate the \vec{N} force term as seen in Eq. 2.84. Therefore, as we would expect for a gravitational source, we will take a mass-current of the form

$$j_1 = 4\pi G\rho(r)v_s = \gamma_0 4\pi G\rho(r)(c\gamma_s - \vec{v}_s\gamma_s), \tag{2.85}$$

where G is the gravitational constant, v_s is the proper velocity of the source, and $\rho(r)$ is its mass density. The subindex in γ_s , as well as in \vec{v}_s , is introduced to distinguish the source's time dilation factor from the particle's in Eq. 2.80.

The scalar part in j_3 , on the other hand, is responsible for generating the relative angular momentum \vec{L} . This would mean having an angular momentum monopole and, once again in complete analogy to the electromagnetic case, such monopoles have not been observed. Therefore, we will set the j_3 source to zero.

With our sources thus defined, Eq. 2.84 becomes

$$\begin{aligned}
\vec{\nabla} \cdot \vec{N} &= -4\pi G\rho(r)\gamma_s, \\
\vec{\nabla} \cdot \vec{L} &= 0, \\
c\partial_0\vec{N} - \vec{\nabla} \times \vec{L} &= 4\pi G\rho(r)\vec{v}_s\gamma_s, \\
\partial_0\vec{L} + c\vec{\nabla} \times \vec{N} &= \vec{0}.
\end{aligned} \tag{2.86}$$

At this point, the only thing left to do in order to get \vec{N} and \vec{L} is solve these equations.

Let us examine \vec{N} first, for which we are going to solve $\vec{\nabla} \cdot \vec{N} = -4\pi G\rho(r)\gamma_s$. This relation can be integrated using the divergence theorem

$$\int_V \vec{\nabla} \cdot \vec{N} dV = \oint_S \vec{N} d\vec{S}. \tag{2.87}$$

Assuming that $\vec{N} = N(r)\hat{r}$ and integrating over a spherical surface of area $4\pi r^2$, we get the expression

$$\vec{N} = -\frac{GM}{r^2}\gamma_s\hat{r}, \tag{2.88}$$

with $M = \int_V \rho(r)dV$, which reminds us of Newton's law. In fact, in the limit that $v_s^2 \ll c^2$, $\gamma_s \rightarrow 1$ and Eq. 2.88 becomes the standard gravitational field.

Now that we have \vec{N} , we can obtain an expression for \vec{L} . This time, however, instead of solving another relation in Eq. 2.86, we are going to use a very convenient result from electromagnetism, $\vec{B} = (\vec{v} \times \vec{E})/c^2$ [20]. Translating this to the gravitational case yields

$$\vec{L} = \vec{v}_s \times \vec{N}. \quad (2.89)$$

Hence, it follows from Eq. 2.88 that the relative angular momentum \vec{L} is

$$\vec{L} = -\frac{GM}{r^2} \gamma_s \vec{v}_s \times \hat{r}, \quad (2.90)$$

where M is the total mass of the source and \vec{v}_s is its relative velocity. Again, when we are in the limit that $v_s^2 \ll c^2$, $\gamma_s \rightarrow 1$. We thus see that \vec{L} is generated by a massive source in movement.

Therefore, having computed the new expressions for \vec{N} and \vec{L} , the gravitational force in Eq. 2.80 takes the form

$$m\dot{v}\gamma_0 = mc\gamma\vec{N} \cdot \vec{v} + m\gamma \left[-\frac{GM}{r^2} \gamma_s c^2 \hat{r} + \vec{v} \times \left(-\frac{GM}{r^2} \gamma_s \vec{v}_s \times \hat{r} \right) \right]. \quad (2.91)$$

Note that the relative velocity \vec{v} , the time dilation factor γ and the mass m refer to the particle, while \vec{v}_s , γ_s and M refer to the gravitational source.

Before moving on to the next chapter, we should pause and look at the implications of the gravitational force we derived together with Eqs. 2.88 and 2.90. We just saw that a gravitational source of total mass M will generate both a field \vec{N} – comparable to a Newtonian gravitational field – and an angular momentum field \vec{L} that is proportional to its velocity. If we take a particle of mass m travelling with velocity \vec{v} , it will experience a force that is the sum of a central force (proportional to \vec{N}) towards the source and a second force perpendicular to both the particle's velocity and the angular momentum field \vec{L} . This will happen whenever the source is rotating with a tangential velocity \vec{v}_s . However, if the source is at rest, that means if $\vec{v}_s = 0$, it will not generate any angular momentum, and thus the only term contributing to the total gravitational force will be \vec{N} .

Having thus derived the gravitational force we were looking for and after computing the expressions of \vec{N} and \vec{L} , we are ready to move forward with the numerical implementation of the force.

Chapter 3

Numerical implementation of the force

As stated in the Introduction, our main objective is to study the effect that the force derived in Sect. 2.3 has on orbits. Motivated by the Milky Way’s plane of satellites problem, we are going to implement this force on a number of satellite galaxies orbiting around our Galaxy. A comparison between the orbits computed using the gravitational force from space-time algebra and those computed with the standard Newtonian force will give us information about the effect of the $\vec{v} \times \vec{L}$ term in Eq. 2.80.

In this chapter we will first describe our simulation, from the specific model we used to the way the force is implemented. We will then be able to show the results obtained from running the simulations and discuss the effect that the gravitational force derived within STA seems to have on the orbits. Finally, we will end by giving some suggestions for future explorations on the topic.

3.1 Simulation

Our simulation comprises a number of test particles that characterize the satellite galaxies, orbiting around a simplified model of the Milky Way. The randomly generated test particles will be isotropically distributed on a sphere around the Galaxy, and we will then let them orbit for 10 Gyr, both under the influence of a Newtonian gravitational force and the force derived within STA, which will allow us to compare the orbits. Since the system is considered to be collisionless, the trajectories of these particles will solely be governed by the Milky Way’s smooth gravitational potential. We will therefore use the leapfrog integrator to compute the orbits, as suggested in [21]. More details on this will be given in what follows.

Overall, there are four steps on our implementation: simulating the Milky Way; generating the test particles, by assigning a random initial position and an accordant initial velocity to each; computing the trajectories, both with the Newtonian force and the STA gravitational force; and comparing the orbits produced by each force. A basic diagram illustrating the implementation of the code is shown in Figure 3.1.

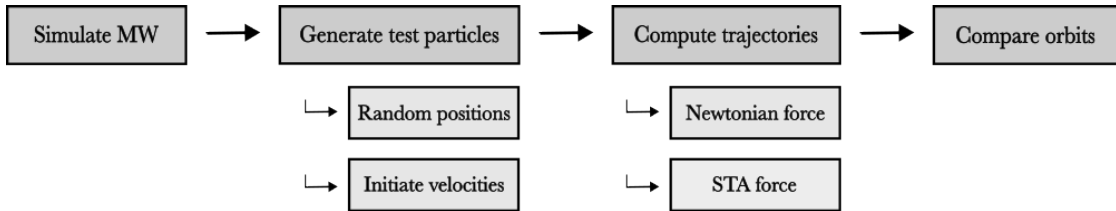


Figure 3.1: Diagram showing the structure of the code. There are four steps for the implementation: simulation of the Milky Way, creation of test particles, computation of trajectories and comparison of orbits. When creating the particles, positions and velocities have been assigned. The trajectories are computed using a Newtonian force and the force derived within STA.

These steps will be explained throughout this section. Should the reader not be interested in an in-depth (and rather tedious) description of the simulation, they are encouraged to jump to the discussion of the results in Sect. 3.2.

3.1.1 Simulating the Milky Way

Let us begin with the first step, creating a simplified model of the Milky Way. As was mentioned, it is the potential of the Galaxy that we are interested in, this will give us the acceleration of the test particles. Our Milky Way model consists of the following elements: a black hole, a bulge of stars, a dark matter halo and an axisymmetric disk of stars. The total potential is thus given by

$$\phi_{\text{MW}}(R, z) = \phi_{\text{bh}}(r) + \phi_{\text{bulge}}(r) + \phi_{\text{dm}}(r) + \phi_{\text{disk}}(R, z; L_z). \quad (3.1)$$

We will now look at each contribution:

- The black hole’s potential is that of a point mass, given by

$$\phi_{\text{bh}}(r) = \frac{-GM_{\text{bh}}}{r}, \quad (3.2)$$

where G is the gravitational constant and M is the total mass.

- The bulge of stars has a potential described by Hernquist’s profile [22] (see Appendix B.1), yielding

$$\phi_{\text{bulge}}(r) = \frac{-GM_{\text{bulge}}}{r + a}, \quad (3.3)$$

where a is a scale length. This potential leads to rosette-like orbits.

- The dark matter halo can also be characterized by Hernquist’s model, so its potential is similarly given by Eq. 3.3.
- The disk of stars consists of a thin and a thick part. As [23] suggests, the potential of a disk at rest is given by

$$\begin{aligned} \phi_{\text{disk},0}(R, z) &= \phi_{\text{thick}}(R, z) + \phi_{\text{thin}}(R, z) = \\ &= \frac{-GM_{\text{thick}}}{\left(R^2 + \left[a_{\text{thick}} + \sqrt{z^2 + b_{\text{thick}}^2}\right]^2\right)^{1/2}} + \frac{-GM_{\text{thin}}}{\left(R^2 + \left[a_{\text{thin}} + \sqrt{z^2 + b_{\text{thin}}^2}\right]^2\right)^{1/2}}, \end{aligned} \quad (3.4)$$

with $R^2 = x^2 + y^2$. This time the potential is not spherical anymore, and thus one has to take into account an additional scale width b for the z -axis. However, since we are dealing with a rotating disk, we need to add a contribution in order to have an effective potential $\phi_{\text{disk}}(R, z; L_z)$ [24]. For an angular momentum $L_z = M_{\text{disk}}v_t r$, the potential becomes

$$\phi_{\text{disk}}(R, z; L_z) = \phi_{\text{disk},0}(R, z) + \frac{L_z^2}{2R^2} = \phi_{\text{disk},0}(R, z) + \frac{(Mv_t r)^2}{2R^2}, \quad (3.5)$$

where v_t is the tangential velocity of the disk and r is its radius.

The values used to compute the potential are specified in Table 3.1, and have been taken from [23] and [25]. In order to determine the angular momentum of the disk, we have used $v_t = 220 \text{ km s}^{-1}$ and $r = 12 \text{ kpc}$.

Body	M / M_{\odot}	a / kpc	b / kpc
Black hole (Sagittarius A*)	$4 \cdot 10^6$	—	—
Bulge of stars	$4.5 \cdot 10^9$	4	—
Dark matter halo	10^{12}	200	—
Thick disk of stars	$3900 \cdot 10^7$	2.6	0.8
Thin disk of stars	$3900 \cdot 10^7$	5.3	0.25

Table 3.1: Mass and scale parameter values used for the modelling of the Milky Way, with masses given in solar mass units and scale parameters given in kpc.

3.1.2 Generating the test particles

Having created the potential, the next step would be to place some test particles in it, which are characterized by their initial position and velocity.

We start by assigning to each particle a random position (r, θ, ϕ) in spherical coordinates, with $r \in [1, 31] \text{ kpc}$ the distance to the center of the Galaxy, $\theta \in [0, \pi]$ the inclination angle and $\phi \in [0, 2\pi)$ the azimuthal angle. We chose that particular interval for the distance r because we want to include orbits that are close to the center, where the effect of the force is the biggest, as well as some others that are at typical distances. For example, the Sagittarius dwarf galaxy is lying at a distance of $\sim 24 \text{ kpc}$ from the center [26], and the Canis Major dwarf galaxy is at a distance of 8.0 kpc [27]. In reality the majority of dwarf galaxies lie a bit further from our Galaxy, but we will see in Sect. 3.2 that the effect of the $\vec{v} \times \vec{L}$ term is the most appealing to us at small distances.

Initial velocities are assigned according to the specific positions of the particles. In order to ensure closed trajectories, the magnitude of the velocity is given by the orbital speed $v_0 = \sqrt{GM(r)/r}$. Then, we assign a random direction in the plane perpendicular to the position vector.

Now that the Milky way is simulated and the particles have been assigned initial positions and velocities, we are ready to compute the orbits.

3.1.3 Orbit integration

The orbits are computed using the leapfrog algorithm [21, 28]. This is a second-order integrator that allows an accurate integration of orbits, as opposed to the more simple Euler method, which performs quite poorly in practice. The leapfrog algorithm is based on updating the positions \vec{x} and velocities \vec{v} of a particle at interleaved timesteps via

$$\begin{cases} \vec{x}_{n+1} = \vec{x}_n + \vec{v}_{n+1/2} \delta t \\ \vec{v}_{n+3/2} = \vec{v}_{n+1/2} + \vec{a}(\vec{x}_{n+1}) \delta t, \end{cases} \quad (3.6)$$

where δt is the interval between each timestep and $n = 0, 1, 2, \dots, N$ is the step number. For a more thorough description of the algorithm and a comparison to the first-order Euler algorithm, see Appendix B.2.

For our case, we are going to integrate the orbits for a total time of 10Gyr, the estimated age of our Galaxy [25]. Specifically, we update positions and velocities every $\delta t = 0.05$ Myr for a total of $N = 200000$ times. These numbers can be modified depending on the precision we are seeking.

The orbits are computed twice: first using a Newtonian acceleration \vec{a}_N and then using the acceleration produced by the STA gravitational force \vec{a}_{STA} . For the computation of Newtonian orbits, we determine the acceleration using that $\vec{a}_N = -\vec{\nabla}\phi_{\text{MW}}$, with ϕ_{MW} given by Eq. 3.1. It is now straightforward to obtain the trajectories by calculating the positions at each timestep using Eq. 3.6.

For the implementation of the STA force there are some things we must take into account. While every element in the Milky Way contributes to the \vec{N} term in Eq. 2.80, we see in Eq. 2.91 that the $\vec{v} \times \vec{L}$ term depends on the velocity of the source \vec{v}_s . Thus, the only element contributing to this force term will be the rotating disk, with its tangential velocity v_t . Moreover, we can simplify Eq. 2.91 by noting that both the velocities of the particles — of order $\sim 10^5 \text{ m s}^{-1}$ — and the velocity of the disk — we use $v_t = 220 \text{ km s}^{-1}$ — satisfy $v^2 \ll c^2$ and $v_s^2 \ll c^2$, so we have that $\gamma \rightarrow 1$ and $\gamma_s \rightarrow 1$. Therefore, the \vec{N} term is completely equivalent to the Newtonian force.

Noting that Eq. 2.91 characterizes a proper quantity, the relative acceleration yields

$$\vec{a}_{\text{STA}} = \vec{a}_N c^2 + \vec{v} \times (-\vec{\nabla}\phi_{\text{disk}} v_t \hat{z}). \quad (3.7)$$

However, the second term's contribution is too small to observe its effect on the orbits. What we do is introduce a parameter ξ that we can adjust in order to increase the effect. It is convenient to multiply Eq. 3.7 by $1/c^2$, so we keep the first term equivalent to the Newtonian force. Thus, what we are implementing in practice is

$$\frac{\vec{a}_{\text{STA}}}{c^2} = \vec{a}_N + \frac{\xi}{c^2} \vec{v} \times (-\vec{\nabla}\phi_{\text{disk}} v_t \hat{z}). \quad (3.8)$$

Using the leapfrog algorithm through Eq. 3.6, we once again determine the positions at each timestep and obtain the orbits that the STA acceleration leads to.

3.1.4 Comparing the orbits

Figure 3.2 depicts the trajectories of three test particles orbiting around the Milky Way, where for illustrative purposes we use $\xi = 20000$ to strengthen the effect of the $\vec{v} \times \vec{L}$. In order to avoid complicated figures, only the last 2.5 Gyr are plotted. Comparing the Newtonian orbits to the STA orbits, we see that the particle that is closer to the center has a slightly different angle as seen from above (xy -plane). In fact, this variation is also manifest in the third column (yz -plane).

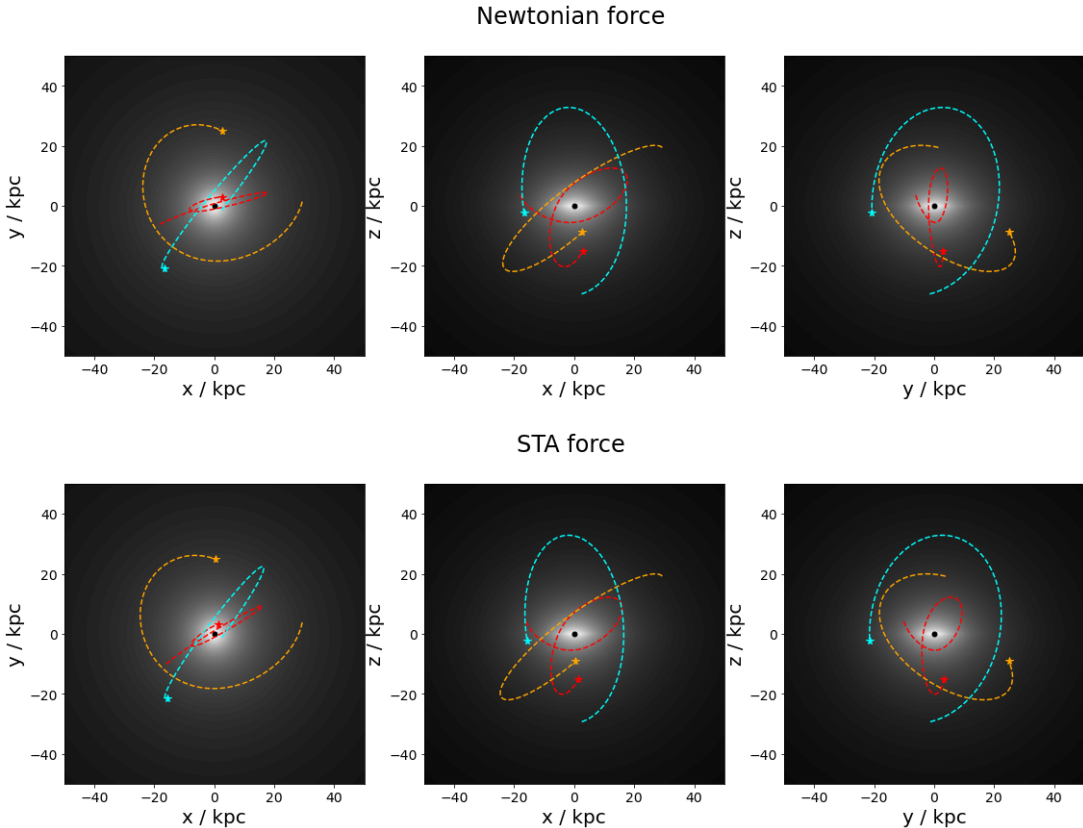


Figure 3.2: Last 2.5 Gyr of three test particles orbiting around the Milky Way. Orbits have been computed using the standard Newtonian force (*top panels*) and the gravitational force derived from STA (*bottom panels*). We have used $\xi = 20000$ for the computation of the STA orbits. Plots show the view of the xy -plane (*left*), the xz -plane (*middle*) and the yz -plane (*right*).

However, it is not so easy to observe the difference between the effect of each gravitational force at plain sight — there is not much to be said about the other two particles' orbits. This requires a careful examination of the difference between final positions, which we can do by representing the particles in the phase space, as shown in Figure 3.3. For instance, with the help of the vertical black line, we see that the particle in red — corresponding to the red orbit in Figure 3.2 — had indeed rotated its orbit, with a shift in the azimuth angle (and a slight variation in the inclination).

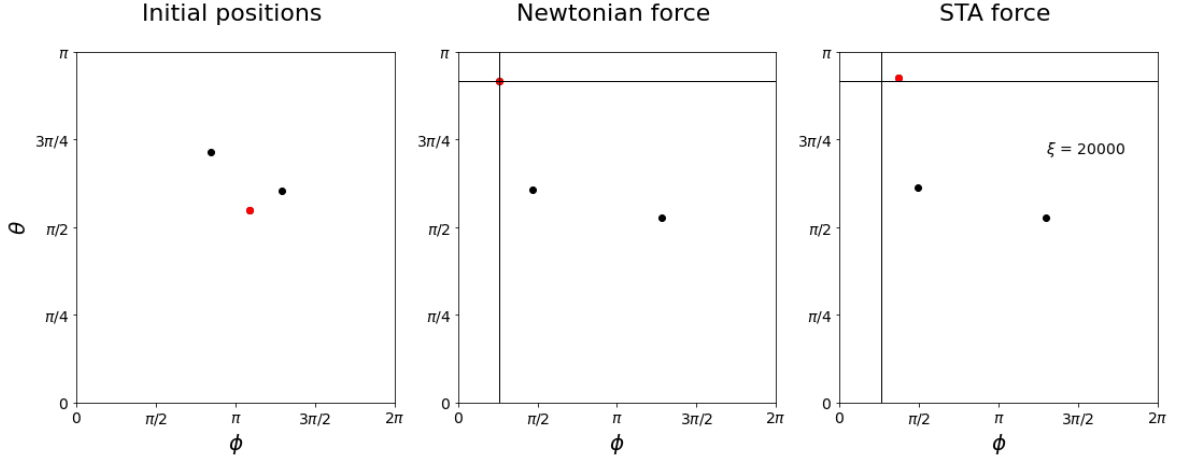


Figure 3.3: Particles’ positions at the beginning of the simulation (*left*), and after orbiting for 10Gyr with a Newtonian acceleration (*middle*) vs. the STA acceleration (*right*) with parameter $\xi = 20000$.

Thus, a proper analysis of the effect of the $\vec{v} \times \vec{L}$ term can be done by measuring $\Delta\phi$ and $\Delta\theta$ for each particle. Regarding their physical interpretation, a shift in the azimuth angle ϕ means that the orbits are rotating in the xy -plane — which can be understood as a precession —, while a shift in the inclination θ might imply an orientation towards a plane — comparable to the Milky Way’s plane of satellites. This will be elaborated upon throughout the discussion of the results.

In this example we have used $\xi = 20000$ in order to be able to observe the rotation of the orbits in Figure 3.2. As we will see in the next section this is an exceedingly high value, as it leads to rather chaotic orbits. In the following we will use lower values that still cause a measurable effect, while trying to keep the orbits stable.

3.2 The effect of the $\vec{v} \times \vec{L}$ term

As we saw in Sect. 3.1.4, an adequate analysis of the orbits requires determining the difference between the final positions that the two forces lead to. For that, we compare the azimuth angle ϕ and the inclination θ for each particle, measuring the shifts $\Delta\phi$ and $\Delta\theta$. We then study their dependence with the distance to the center r .

Before doing this we should, however, think about the choice of ξ in Eq. 3.8. We want to find a balance between having a big enough contribution so that the effect is measurable, and having consistent orbits. We assess this by measuring $|\vec{N}|/(|\vec{N}| + |\xi \vec{v} \times \vec{L}/c^2|)$ through time. This coefficient quantifies the contribution of the $\vec{v} \times \vec{L}$ term normalized with respect to the \vec{N} term. In particular, when ξ is too big, this term becomes increasingly important compared to \vec{N} , meaning that the orbits lose their stability, and the coefficient will eventually drop. Hence, we are interested in parameters ξ that keep the coefficient stable in time. But this is not the only criterion we must follow in order to set a limit on ξ .

Figure 3.4 shows the evolution of $|\vec{N}|/(|\vec{N}| + |\xi \vec{v} \times \vec{L}/c^2|)$ for different parameters, averaged over 200 test particles. We see that for both $\xi = 20000$ and $\xi = 2000$ the coefficient keeps stable through time. However, the error bars for $\xi = 20000$ deviate significantly from the average, meaning that different particles will have very different coefficients and the effect of the $\vec{v} \times \vec{L}$ term will fluctuate a lot. Having consistent orbits thus requires a coefficient that is both constant in time and has a small variation from the average, such as for the $\xi = 2000$ case.

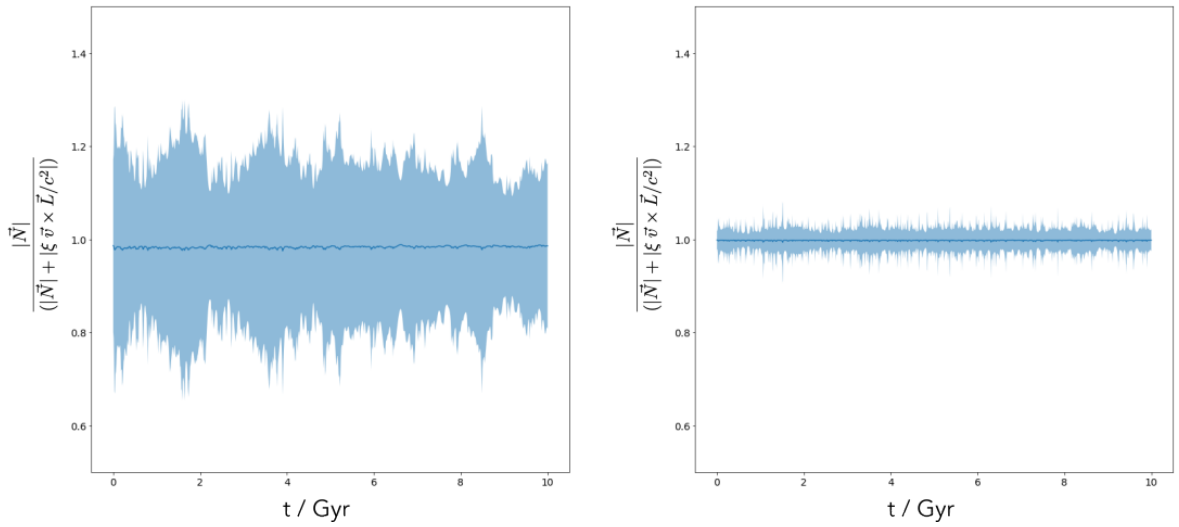


Figure 3.4: Evolution of $|\vec{N}|/(|\vec{N}| + |\xi \vec{v} \times \vec{L}/c^2|)$ in time, averaged over 200 test particles, for $\xi = 20000$ (*left*) and $\xi = 2000$ (*right*). Error bars are shown in light blue.

Let us thus examine the 200 orbits computed with $\xi = 2000$. The correlation between the shifts $\Delta\phi$ and $\Delta\theta$ and the distance of the particles to the center of the Galaxy r is represented in Figure 3.5.

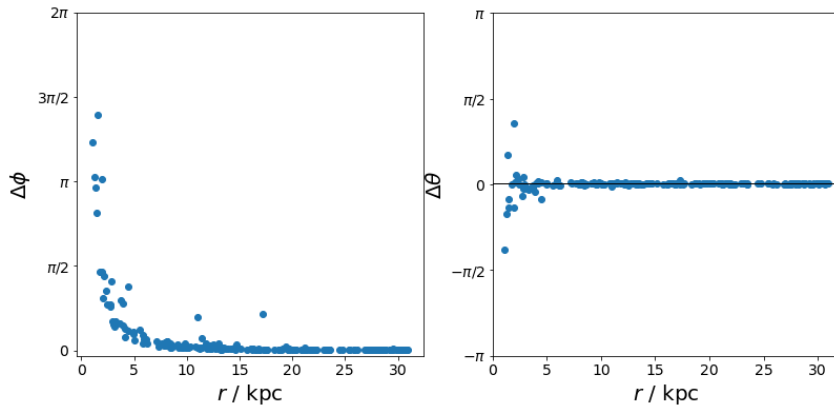


Figure 3.5: $\Delta\phi$ (*left*) and $\Delta\theta$ (*right*) depending on the distance to the center r . Number of particles: 200. $\xi = 2000$.

On the one hand, we see that there is in general — except for the numerical noise at small distances — no variation in the inclination angle θ , which means that orbits have the same inclination when computed with the Newtonian acceleration or computed with the STA acceleration. Therefore, we can conclude that the gravitational force derived from spacetime algebra does not have a tendency to align orbits, and hence bears no relation to the Milky Way’s plane of satellites.

On the other hand, the $\vec{v} \times \vec{L}$ term does have an effect on the azimuth angle ϕ . As was hinted in Sect. 3.1.4, orbits under the influence of this force experience a rotation in the xy -plane as compared to Newtonian orbits. This effect is significant at lower distances, as can be seen in Figure 3.5. We can try to fit the data as

$$\Delta\phi = \frac{\alpha GMv_t}{r^2}, \quad (3.9)$$

where α is the fitting parameter. For this it is convenient to represent the data in logarithmic scale, as has been done in Figure 3.6, and fit it linearly as $\log \Delta\phi = b + m \log r$, with $b = \log(\alpha GMv_t)$. Hence, we get α from the intercept. Doing this for $\xi = 2000$ yields $\alpha = (3021 \pm 714)$.

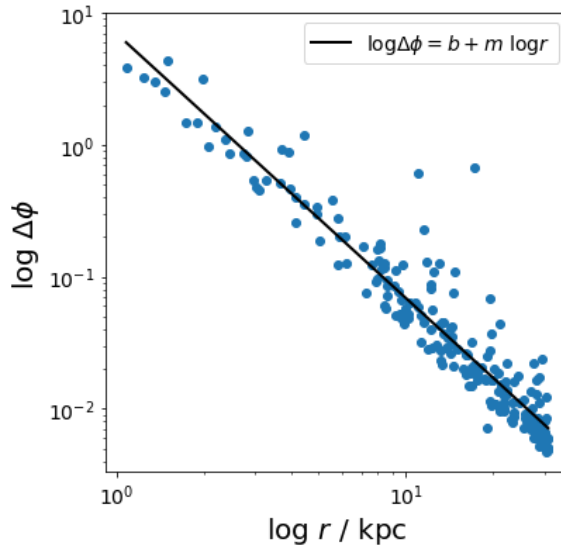


Figure 3.6: Correlation between $\Delta\phi$ and r in logarithmic scale. Number of particles: 200. $\xi = 2000$. The black line represents the linear fit $\log \Delta\phi = b + m \log r$, where $b = \log(\alpha GMv_t)$.

In order to further study this effect we can compute the orbits for different parameters ξ and obtain α . We do this for $500 \leq \xi \leq 3000$, increasing in steps of 500. A value bigger than $\xi = 3000$ gives an effect that fluctuates too much from particle to particle — an example of this is shown in Figure B.8 for $\xi = 3500$, where we see that the fit is not sufficiently good, since there are a lot of particles that deviate from the curve. With this in mind, Figure 3.7 shows the correlation between the fitting parameter α and the STA parameter ξ (see Table B.1 for the corresponding values, obtained by fitting the data in Figures B.3 – B.7). A linear fit gives $\alpha = (1.4 \pm 0.2)\xi + (178 \pm 272)$. Note that if we extrapolate from the linear fit, for

$\xi = 0$ we find $\alpha(0) = 178 \pm 272$. At this point we should see no rotation in the orbits, since the only term present in the gravitational force is the Newtonian acceleration — this falls within the margin of error of our fit. Alternatively, we can also force the fit to go through the origin, obtaining $\alpha = (1.50 \pm 0.14)\xi$.

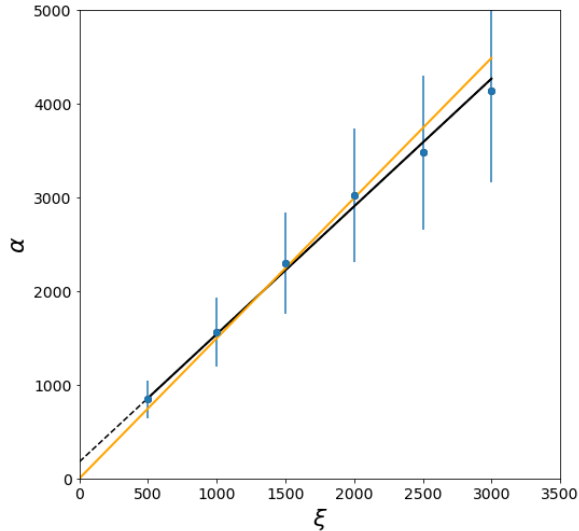


Figure 3.7: Correlation between α and the STA parameter ξ . The black line shows a linear fit, and the dashed line extrapolates the fit to $\xi = 0$. Additionally, the orange line represents the linear fit when we force the line to go through the origin.

All things considered, our work fails to give an explanation for the plane of dwarf galaxies — no significant difference has been found on the inclination angle of the orbits of the test particles. Nevertheless, the results interestingly reveal that the $\vec{v} \times \vec{L}$ term causes orbits to rotate in the disk plane, with the shift in the angle increasing at small distances. We believe that this may be related to orbit precession, which Newtonian gravity is not able to explain properly. This will need to be studied in a more exhaustive investigation of the effect.

In order to get an idea of the magnitude of this effect, it might be interesting to consider some examples. If we get realistic and consider $\xi = 1$, which is the case where the Newtonian and the $\vec{v} \times \vec{L}$ term have the same weight on the force, we can extrapolate that $\alpha(\xi = 1) = 1.50$ from the linear fit in Figure 3.7 and using Eq. 3.9 we see that a test particle at a distance $r = 10\text{kpc}$ from the center of the Galaxy would experience a shift of $\Delta\phi = 7 \cdot 10^{-7}''$. In order to see a more meaningful effect we would have to go to small radii — at $r = 1\text{ly}$, for instance, the effect would be $\Delta\phi = 0.22^\circ$.

3.3 Discussion and further explorations

In this chapter we have discussed the implementation of the gravitational force derived within the framework of spacetime algebra. Comparing the resulting orbits to the ones integrated using the standard Newtonian force, we have been able to analyze the effect of the additional $\vec{v} \times \vec{L}$ term and find that it causes orbit precession. However, it is important to

be judicious in the interpretation of this effect, given that our data may be influenced by a number of limitations.

One of our code’s weaknesses concerns the level of precision of the results. The orbits were integrated using timesteps of $\delta t = 0.05$ Myr. Higher precision could have been reached by taking smaller timesteps; however, that would have required an unreasonably high computation time — integrating the trajectories of 200 particles during 10 Gyr with timesteps $\delta t = 0.05$ Myr took ~ 72 h. This can be dealt with by introducing variable timesteps [29, 30], which improves the performance of the code by assigning a different timestep to each particle, depending on their distance to the center of the Galaxy. In this way, most of the computation time is employed in particles near the center, which require very small timesteps, whereas more distant orbits can be integrated in less time using big timesteps.

An additional complication arises from forces going to infinity very close to the center of the Galaxy, leading to numerical divergences. We could overcome this issue with the implementation of force softening [21, 31], therefore getting more accuracy in our results at small distances.

We believe that these two numerical tricks will substantially improve the precision of the integrated trajectories at small distances, diminishing the numerical noise in $\Delta\theta$ (seen in Figure 3.5). Thus, these techniques are expected to provide more reliable results. They remain to be implemented in future analyses.

With our current results we have concluded that the $\vec{v} \times \vec{L}$ term of the force makes orbits precess in the disk plane. Future explorations on the topic should focus on further studying this precession in order to validate our conclusions. In particular, it would be an interesting idea to test the effect of the force at planetary level, such as in the Solar System, and see whether our results support Christiansen’s [19] findings regarding Mercury’s orbital precession within the framework of spacetime algebra. Assuming STA manages to accurately predict the precession of elliptical orbits, the framework would prove advantageous over the Newtonian theory of gravity, which does not succeed in giving an appropriate description of precession.

In conclusion, it is crucial to bear in mind the several limitations of our implementation, and therefore we should treat the obtained results with the utmost caution. However, the code has in general an adequate performance, and this first implementation of the STA gravitational force serves at least as a base for future studies, having given an initial idea of what the effect of the $\vec{v} \times \vec{L}$ term is.

Chapter 4

Conclusions

Thanks to its simple description of physics, spacetime algebra has lately gained increasing popularity within the scientific community. In many areas such as crystallography [32] — with its simple handling of point symmetry groups — or quantum mechanics [33] — where it provides a geometric interpretation of Pauli and Dirac matrices —, the framework has proven to substantially simplify physics. What is more, spacetime algebra entails a unified language for mathematics, since it integrates all methods required to formulate physical concepts. Nonetheless, to the best of our knowledge the theory has primarily been developed from a theoretical viewpoint, and its practical implications have not been tested numerically. With the main purpose of exploring the effects of the gravitational force derived within STA as an alternative to the standard Newtonian force, in this work we have investigated spacetime algebra as a tool to describe gravity.

In order to do so, first we have given a fully theoretical approach to the framework, starting from an introduction to the more general geometric algebra. We have been able to provide a comprehensive description of some general notions, such as complex numbers or Lorentz transformations, from mere geometric considerations. The implications of this are remarkable: we find that many physical concepts are inherently geometrical in nature, which significantly simplifies physics' formulation. Having thus built the tools we need, we have derived a gravitational force within the framework of spacetime algebra, given by Eq. 2.91, which differs from the Newtonian gravitational force by an additional $\vec{v} \times \vec{L}$ term. We have then implemented the force on a system consisting of 200 randomly generated test particles orbiting around a simplified model of the Milky Way. Additionally computing the orbits using a standard Newtonian force, we have finally been able to compare the orbits produced by each force, which has shed some light on what the extra term in the gravitational force does.

The results from this study point towards the idea that the $\vec{v} \times \vec{L}$ term causes orbit precession. This means that, as opposed to Newtonian gravity, spacetime algebra might be able to properly describe precession, as general relativity does. However, there are many nuances to this statement, and a lot of investigation remains to be carried out into this matter.

The present work entails no more than a preliminary exploration of a much more ambitious study. The importance of the obtained results lies on having revealed the value of implementing this alternative force rather than the standard Newtonian force. So far we have

seen that the idea is feasible and that it is worth examining the precession effect in a more detailed study. Moreover, the implementation still presents several limitations that need to be overcome in future stages of the development of the work, such as introducing variable timesteps or force softening techniques.

In conclusion, spacetime algebra might prove to be a valuable tool to formulate gravity, as it already is for the description of many branches in physics, like electromagnetism or quantum mechanics. For this reason, and because it allows an uncomplicated and coordinate-free formulation of many fundamental notions, we want to restate the educational value of the framework and its benefits as a unified mathematical language.

Appendix A

Conserved quantities within classical field theory

This appendix aims to illustrate how the framework of spacetime algebra simplifies the derivation of energy and angular momentum conservation. In fact, this is inherent to the geometric structure of the framework, in classical field theory, as it will be seen, requires a much longer derivation.

Let us assume a Lagrangian density that depends on the fields $\phi_i(x^\mu)$ as follows:

$$\mathcal{L} \equiv \mathcal{L}(\phi_i, \partial_\mu \phi_i).$$

We have a continuous variation in spacetime such that the fields transform as

$$\phi_i(x^\nu) \rightarrow \phi_i(x^\nu + \varepsilon^\nu) = \phi_i(x^\nu) + \varepsilon^\nu \partial_\nu \phi_i(x^\nu) + \mathcal{O}(\varepsilon^2),$$

where we identify $\delta\phi_i(x^\nu) = \varepsilon^\nu \partial_\nu \phi_i(x^\nu)$.

Now we have to look at the variation of the Lagrangian,

$$\delta\mathcal{L} = \frac{\partial\mathcal{L}}{\partial\phi_i} \delta\phi_i + \frac{\partial\mathcal{L}}{\partial(\partial_\mu\phi_i)} \delta\partial_\mu\phi_i = \frac{\partial\mathcal{L}}{\partial\phi_i} \delta\phi_i + \frac{\partial\mathcal{L}}{\partial(\partial_\mu\phi_i)} \partial_\mu\delta\phi_i. \quad (\text{A.1})$$

At this point we can use the Euler-Lagrange equations of motion,

$$\frac{\partial\mathcal{L}}{\partial\phi_i} - \partial_\mu \left(\frac{\partial\mathcal{L}}{\partial(\partial_\mu\phi_i)} \right) = 0.$$

Therefore, Eq. A.1 becomes

$$\begin{aligned} \delta\mathcal{L} &= \partial_\mu \left(\frac{\partial\mathcal{L}}{\partial(\partial_\mu\phi_i)} \right) \delta\phi_i + \frac{\partial\mathcal{L}}{\partial(\partial_\mu\phi_i)} \partial_\mu\delta\phi_i = \partial_\mu \left(\frac{\partial\mathcal{L}}{\partial(\partial_\mu\phi_i)} \delta\phi_i \right) = \\ &= \partial_\mu \left(\frac{\partial\mathcal{L}}{\partial(\partial_\mu\phi_i)} \varepsilon^\nu \partial_\nu\phi_i \right). \end{aligned} \quad (\text{A.2})$$

On the other hand one can write the variation of the Lagrangian as

$$\delta\mathcal{L} = \frac{\partial\mathcal{L}}{\partial x^\mu} \delta x^\mu = \frac{\partial\mathcal{L}}{\partial x^\mu} \delta_\nu^\mu \varepsilon^\nu = \partial_\mu (\mathcal{L} \delta_\nu^\mu \varepsilon^\nu), \quad (\text{A.3})$$

since the delta function and the infinitesimal variation do not change the derivative when included in it.

It is now a matter of combining Eqs. A.2 and A.3 into

$$\partial_\mu \left(\left[\frac{\partial \mathcal{L}}{\partial(\partial_\mu \phi_i)} \partial_\nu \phi_i - \mathcal{L} \delta_\nu^\mu \right] \varepsilon^\nu \right) = 0.$$

Defining here the energy-momentum tensor T_ν^μ , we find that

$$\partial_\mu \left(\frac{\partial \mathcal{L}}{\partial(\partial_\mu \phi_i)} \partial_\nu \phi_i - \mathcal{L} \delta_\nu^\mu \right) = \partial_\mu T_\nu^\mu = 0.$$

T_ν^μ is thus a conserved current. We just derived that spacetime homogeneity leads to energy and momentum conservation. Time translations with $\nu = 0$ lead to energy conservations and space translations with $\nu = j$ with $j \in 1, 2, 3$ lead to momentum conservation.

One can also apply a Lorentz transformation to the spacetime coordinates. Expanding the Lorentz transformation gives $\Lambda_\nu^\mu = \delta_\nu^\mu + \omega^{\mu\nu} + \mathcal{O}(\omega^2)$. The fields thus change as

$$\phi_i(x^\mu) \rightarrow \phi_i(\Lambda^{\mu\nu} x_\nu) = \phi_i(x^\mu + \omega^{\mu\nu} x_\nu) = \phi_i(x^\mu) + \omega^{\mu\nu} x_\nu \partial_\mu \phi_i(x^\mu) + \mathcal{O}(\omega^2),$$

where $\omega^{\mu\nu}$ is the infinitesimal Lorentz transformation.

We start by writing the variation of the Lagrangian like before, but this time what we identify as the field deformation is $\delta\phi_i = \omega^{\mu\nu} x_\nu \partial_\mu \phi_i$, so Eq. A.2 will be

$$\delta \mathcal{L} = \partial_\sigma \left(\frac{\partial \mathcal{L}}{\partial(\partial_\sigma \phi_i)} \delta\phi_i \right) = \partial_\sigma \left(\frac{\partial \mathcal{L}}{\partial(\partial_\sigma \phi_i)} \omega^{\mu\nu} x_\nu \partial_\mu \phi_i \right) = \partial_\sigma \left(\frac{\partial \mathcal{L}}{\partial(\partial_\sigma \phi_i)} \frac{1}{2} \omega^{\mu\nu} (x_\nu \partial_\mu \phi_i - x_\mu \partial_\nu \phi_i) \right), \quad (\text{A.4})$$

where we have used that $\omega^{\mu\nu}$ is antisymmetric. Similarly, Eq. A.3 becomes

$$\delta \mathcal{L} = \frac{\partial \mathcal{L}}{\partial x^\sigma} \delta x^\sigma = \frac{\partial \mathcal{L}}{\partial x^\sigma} \frac{1}{2} \omega^{\mu\nu} (\delta_\mu^\sigma x_\nu - \delta_\nu^\sigma x_\mu) = \partial_\sigma \left(\mathcal{L} \frac{1}{2} \omega^{\mu\nu} (\delta_\mu^\sigma x_\nu - \delta_\nu^\sigma x_\mu) \right). \quad (\text{A.5})$$

Combining Eqs. A.4 and A.5 and manipulating the result a bit yields

$$\partial_\sigma \left(\left[\frac{\partial \mathcal{L}}{\partial(\partial_\sigma \phi_i)} \partial_\mu \phi_i - \mathcal{L} \delta_\mu^\sigma \right] x_\nu - \left[\frac{\partial \mathcal{L}}{\partial(\partial_\sigma \phi_i)} \partial_\nu \phi_i - \mathcal{L} \delta_\nu^\sigma \right] x_\mu \right) = 0.$$

Using the definition of T_ν^μ , we get that

$$J_{\mu\nu}^\sigma = T_\mu^\sigma x_\nu - T_\nu^\sigma x_\mu. \quad (\text{A.6})$$

is a conserved quantity, which is the angular momentum.

We have thus derived the conservations of the energy-momentum and the angular momentum within classical field theory.

Appendix B

Numerical implementation

B.1 Hernquist potential

Hernquist's model [22] is described by the following density profile:

$$\rho(r) = \frac{M a}{2\pi r} \frac{1}{(r + a)^3}, \quad (\text{B.1})$$

where M is the total mass and a is a scale length. We can find the potential $\phi(r)$ by integrating Poisson's equation $\nabla^2\phi(r) = 4\pi G\rho(r)$ for Eq. B.1, and for that we can use the Green's function of the Laplacian:

$$\begin{aligned} \phi(r) &= -4\pi G \int_V \frac{1}{4\pi|\vec{r} - \vec{r}'|} \rho(\vec{r}') d^3\vec{r}' = -G \int_0^{2\pi} \int_0^\pi \int_0^r \frac{M a}{2\pi r} \frac{1}{(r + a)^3} \frac{1}{|\vec{r} - \vec{r}'|} r^2 \sin\theta d\theta d\phi dr = \\ &= -GM2a \int_0^r \frac{r}{(r + 1)^3} \frac{1}{|\vec{r} - \vec{r}'|} dr. \end{aligned} \quad (\text{B.2})$$

Solving the integral to get Hernquist's potential

$$\phi(r) = -\frac{GM}{r + a}, \quad (\text{B.3})$$

we can finally obtain the acceleration that such a potential would cause to a test particle using that $\vec{a} = -\vec{\nabla}\phi$, yielding

$$\vec{a} = -\frac{GM}{(r + a)^2} \frac{\vec{r}}{|\vec{r}|}. \quad (\text{B.4})$$

B.2 Leapfrog integrator

An adequate algorithm that integrates the equations of motion of a system, for example for orbit computation, needs to fill some requirements, depending on the type of simulation one is running. For example, for long integrations, it is important that the integrator conserves quantities of motion such as energy or momentum, given that equations of motion do satisfy conservation laws and one should find an integrator that resembles reality as much

as possible. This is the case for the *leapfrog integrator*, in contrast with the simpler Euler method. These two integration algorithms will be compared in the following.

Given a position x and a velocity v at time t , we want to generate new coordinates x' and v' at time $t + \delta t$, where δt is the timestep. The goal is to solve Newton's equations of motion,

$$v = \frac{dx}{dt} \quad (\text{B.5})$$

and

$$a(x) = \frac{F(x)}{m} = \frac{dv}{dt}, \quad (\text{B.6})$$

which Euler approximates by

$$\begin{cases} x_{n+1} = x_n + v_n \delta t \\ v_{n+1} = v_n + a(x_n) \delta t. \end{cases} \quad (\text{B.7})$$

This is a first-order integration algorithm. That means the error per step δt will be proportional to $\mathcal{O}(\delta t^2)$. Thus, the orbits integrated using the Euler method will considerably deviate from the actual curve, unless $\delta t \rightarrow 0$. However, if we update positions and velocities at interleaved time-points,

$$\begin{cases} x_{n+1} = x_n + v_{n+1/2} \delta t \\ v_{n+3/2} = v_{n+1/2} + a(x_{n+1}) \delta t, \end{cases} \quad (\text{B.8})$$

we get the leapfrog integrator, which is second-order, so the error is $\mathcal{O}(\delta t^3)$.

Figure B.1 compares Euler and leapfrog integrators for different time-steps. As $\delta t \rightarrow 0$ the error in the Euler method decreases significantly, and starts to reach the accuracy of the leapfrog integrator.

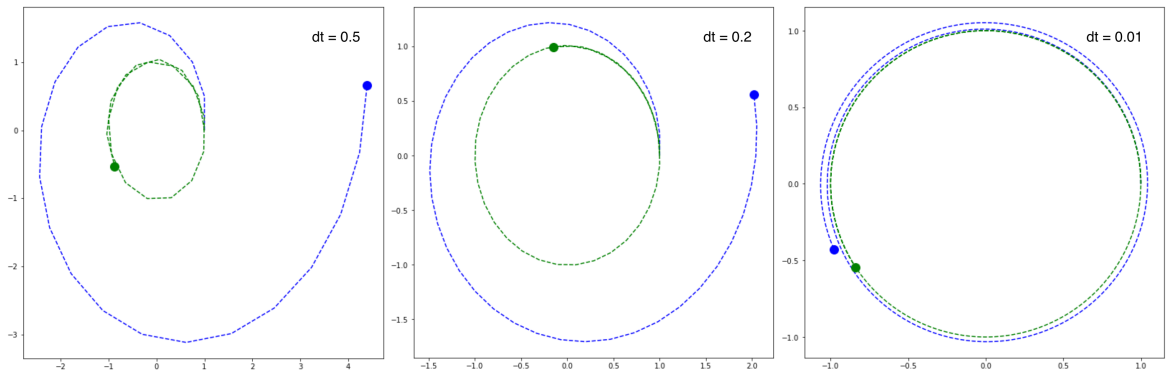


Figure B.1: Orbit integration using the Euler method (blue) and the leapfrog method (green) for different timesteps. From left to right, $\delta t = 0.5$, $\delta t = 0.2$ and $\delta t = 0.01$. We can see that as $\delta t \rightarrow 0$, the error in the Euler method is smaller, and reaches the accuracy of the leapfrog method.

Although accuracy is not the only reason why one would choose the leapfrog integrator over Euler. Time-reversibility is an important feature of the leapfrog algorithm. We want to make sure that when integrating an orbit, and going from (x, v) to (x', v') in a timestep, we can reverse this by going from $(x', -v')$ to $(x, -v)$ in the same time. This means there is energy conservation, since if there were dissipation, then it would not be reversible in time.

It can be checked numerically that the leapfrog integrator conserves energy, while the Euler method does not. Figure B.2 shows each integrator's behaviour if one computes the energy of an orbit at each time-step. The orbit corresponds to an arbitrary test particle orbiting around the Milky Way. The leapfrog integrator (in green) fluctuates within the period of an orbit, but is preserved in time, while in the Euler case (in blue) the particle's energy is slowly dissipated, and it is manifest that the energy conservation is lost. This means the Euler method is not reversible in time.

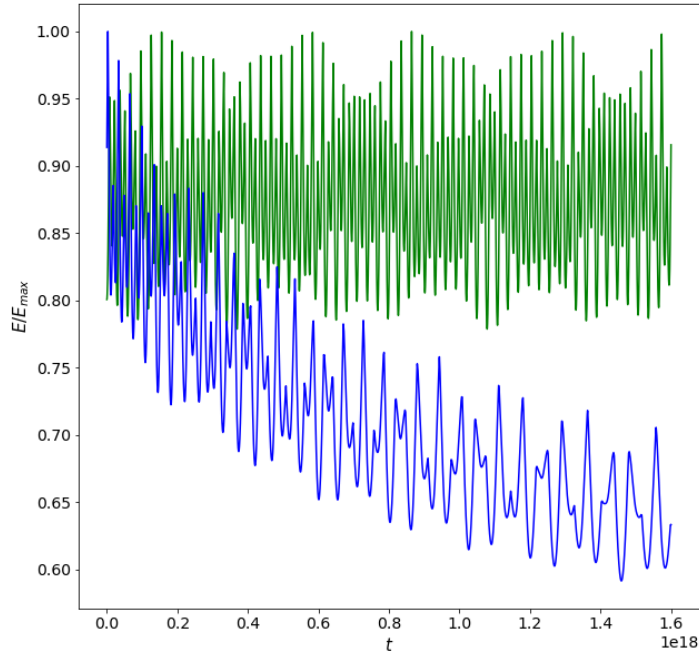


Figure B.2: Energy fraction as a function of time for the leapfrog method (green) and for the Euler method (blue).

The leapfrog algorithm is thus preferred over the Euler algorithm, since it does not require the use of such small timesteps in order to obtain accurate orbits.

B.3 Additional figures

This appendix presents the angle comparisons $\Delta\phi$ and $\Delta\theta$ as a function of the distance r for parameters $500 \leq \xi \leq 3500$.

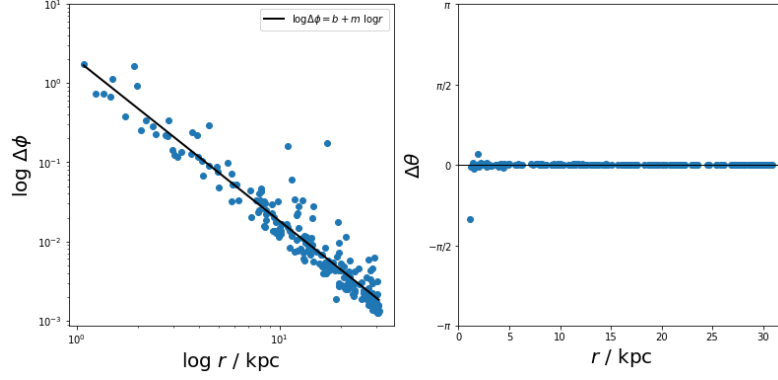


Figure B.3: Correlation between $\Delta\phi$ and r in logarithmic scale (*left*) and $\Delta\theta$ and r (*right*). Number of particles: 200. $\xi = 500$. The black line represents the linear fit $\log \Delta\phi = b + m \log r$, where $b = \log(\alpha GM v_t)$.

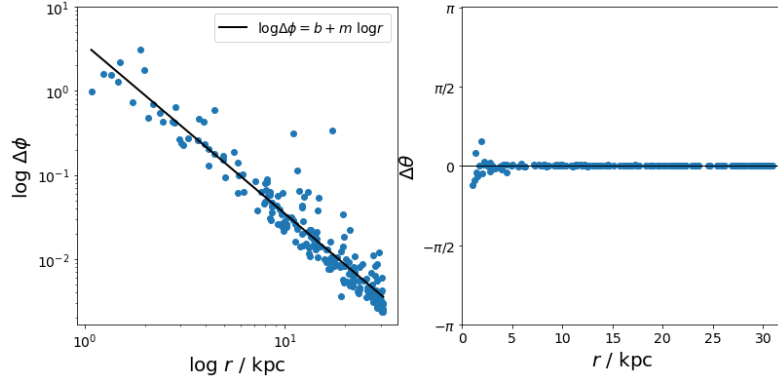


Figure B.4: Correlation between $\Delta\phi$ and r in logarithmic scale (*left*) and $\Delta\theta$ and r (*right*). Number of particles: 200. $\xi = 1000$. The black line represents the linear fit $\log \Delta\phi = b + m \log r$, where $b = \log(\alpha GM v_t)$.

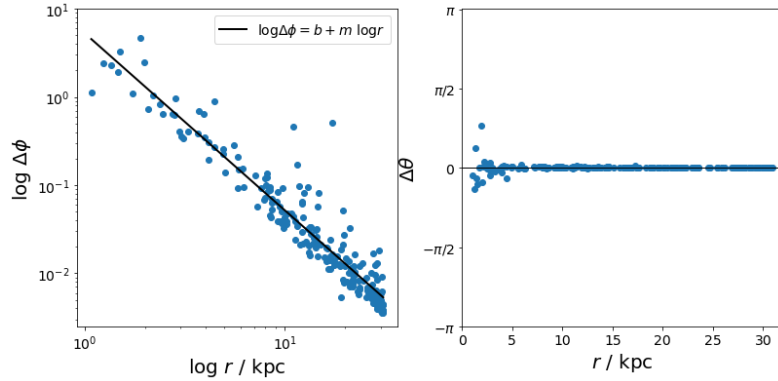


Figure B.5: Correlation between $\Delta\phi$ and r in logarithmic scale. Number of particles: 200. $\xi = 1500$. The black line represents the linear fit $\log \Delta\phi = b + m \log r$, where $b = \log(\alpha GM v_t)$.

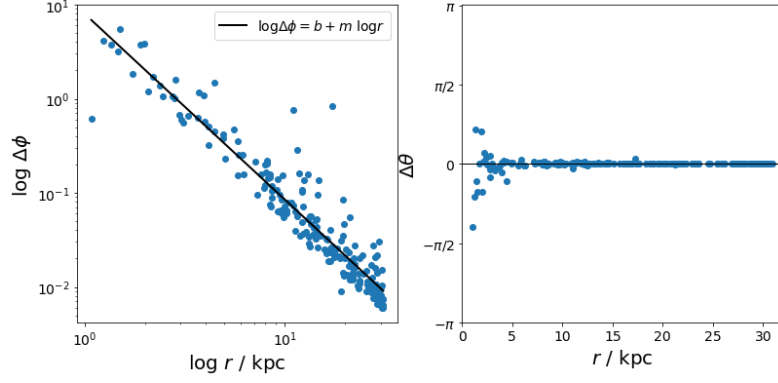


Figure B.6: Correlation between $\Delta\phi$ and r in logarithmic scale (*left*) and $\Delta\theta$ and r (*right*). Number of particles: 200. $\xi = 2500$. The black line represents the linear fit $\log \Delta\phi = b + m \log r$, where $b = \log(\alpha GM v_t)$.

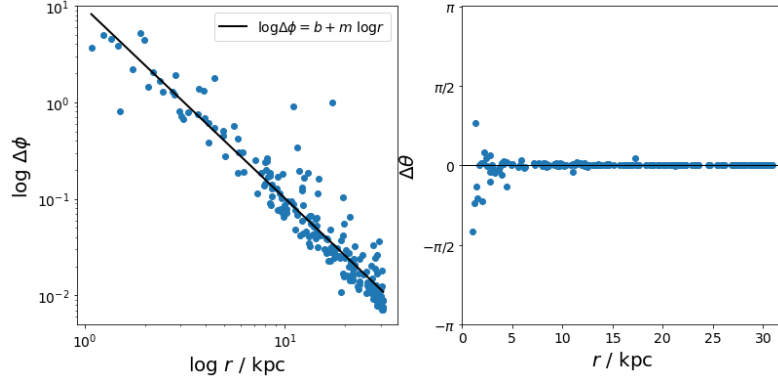


Figure B.7: Correlation between $\Delta\phi$ and r in logarithmic scale (*left*) and $\Delta\theta$ and r (*right*). Number of particles: 200. $\xi = 3000$. The black line represents the linear fit $\log \Delta\phi = b + m \log r$, where $b = \log(\alpha GM v_t)$.

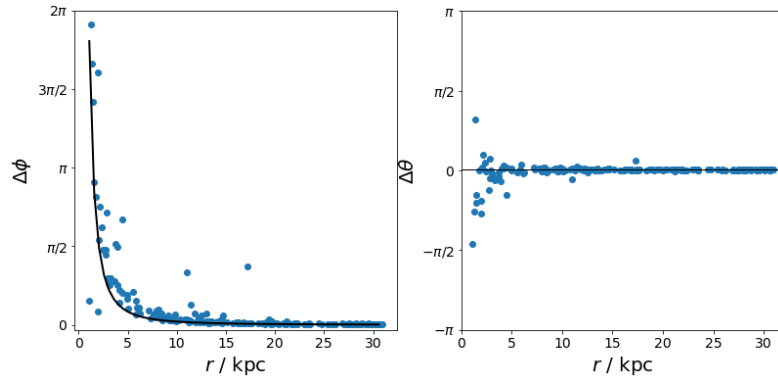


Figure B.8: Correlation between $\Delta\phi$ (*left*) and $\Delta\theta$ (*right*) and the distance to the center r . Number of particles: 200. $\xi = 3500$.

ξ	α	σ_α
500	847	200
1000	1556	368
1500	2294	542
2000	3021	714
2500	3478	823
3000	4138	979

Table B.1: Fitting parameter $\alpha \pm \sigma_\alpha$ for each parameter ξ .

Bibliography

- [1] M. Metz, P. Kroupa, N. I. Libeskind, The Orbital Poles of Milky Way Satellite Galaxies: A Rotationally Supported Disk of Satellites, *The Astrophysical Journal* 680 (1) (2008) 287–294. doi:[10.1086/587833](https://doi.org/10.1086/587833).
- [2] M. Metz, P. Kroupa, H. Jerjen, The spatial distribution of the Milky Way and Andromeda satellite galaxies, *Monthly Notices of the Royal Astronomical Society* 374 (3) (2007) 1125–1145. doi:[10.1111/j.1365-2966.2006.11228.x](https://doi.org/10.1111/j.1365-2966.2006.11228.x).
- [3] D. Lynden-Bell, Dwarf Galaxies and Globular Clusters in High Velocity Hydrogen Streams, *Monthly Notices of the Royal Astronomical Society* 174 (3) (1976) 695–710. doi:[10.1093/mnras/174.3.695](https://doi.org/10.1093/mnras/174.3.695).
- [4] T. Sawala, M. Cautun, C. S. Frenk, J. Helly, J. Jasche, A. Jenkins, P. H. Johansson, G. Lavaux, S. McAlpine, M. Schaller, The Milky Way’s plane of satellites: consistent with Λ CDM (2022). [arXiv:2205.02860](https://arxiv.org/abs/2205.02860).
- [5] R. A. Ibata, G. F. Lewis, A. R. Conn, M. J. Irwin, A. W. McConnachie, S. C. Chapman, M. L. Collins, M. Fardal, A. M. N. Ferguson, N. G. Ibata, A. D. Mackey, N. F. Martin, J. Navarro, R. M. Rich, D. Valls-Gabaud, L. M. Widrow, A vast, thin plane of corotating dwarf galaxies orbiting the andromeda galaxy, *Nature* 493 (7430) (2013) 62–65. doi:[10.1038/nature11717](https://doi.org/10.1038/nature11717).
- [6] S. H. Hansen, A force proportional to velocity squared derived from spacetime algebra, *Monthly Notices of the Royal Astronomical Society: Letters* 506 (1) (2021) L16–L19. doi:[10.1093/mnrasl/slab065](https://doi.org/10.1093/mnrasl/slab065).
- [7] D. Hestenes, Oersted medal lecture 2002: Reforming the mathematical language of physics, *American Journal of Physics - AMER J PHYS* 71 (2003) 104–121. doi:[10.1119/1.1522700](https://doi.org/10.1119/1.1522700).
- [8] W. R. Hamilton, LXXVIII. On quaternions; or on a new system of imaginaries in Algebra : To the editors of the *Philosophical Magazine and Journal* (Jan. 1844). doi:[10.1080/14786444408645047](https://doi.org/10.1080/14786444408645047).
- [9] H. Grassmann, *Die Lineale Ausdehnungslehre Ein Neuer Zweig Der Mathematik*, 1844.
- [10] P. Clifford, Applications of grassmann’s extensive algebra, *American Journal of Mathematics* 1 (4) (1878) 350–358.

- [11] D. Hestenes, Spacetime Physics with Geometric Algebra, American Journal of Physics 71 (07 2003). doi:10.1119/1.1571836.
- [12] D. Hestenes, Space-time Algebra, second edition, 2015. doi:10.1007/978-3-319-18413-5.
- [13] J. Dressel, K. Y. Bliokh, F. Nori, Spacetime algebra as a powerful tool for electromagnetism, Physics Reports 589 (2015) 1–71. doi:10.1016/j.physrep.2015.06.001.
- [14] A. Lasenby, C. Doran, S. Gull, Gravity, gauge theories and geometric algebra, Philosophical Transactions of the Royal Society of London. Series A: Mathematical, Physical and Engineering Sciences 356 (1737) (1998) 487–582. doi:10.1098/rsta.1998.0178.
- [15] C. Doran, A. Lasenby, Geometric Algebra for Physicists, Cambridge University Press, 2003. doi:10.1017/CB09780511807497.
- [16] D. Hestenes, New Foundations for Classical Mechanics, Fundamental Theories of Physics, Springer Netherlands, 1986.
- [17] T. Vold, An introduction to geometric algebra with an application in rigid body mechanics, American Journal of Physics - AMER J PHYS 61 (1993) 491–504. doi:10.1119/1.17201.
- [18] L. D. Landau, E. M. Lifshitz, The Classical Theory of Fields: Volume 2, Pergamon Press Ltd., 1975.
- [19] H. Christiansen, S. H. Hansen, 2023, (in prep.).
- [20] D. J. Griffiths, Electromagnetism for physicists, 2015.
- [21] W. Dehnen, J. I. Read, N-body simulations of gravitational dynamics, The European Physical Journal Plus 126 (5) (may 2011). doi:10.1140/epjp/i2011-11055-3.
- [22] L. Hernquist, An Analytical Model for Spherical Galaxies and Bulges, 356 (1990) 359. doi:10.1086/168845.
- [23] Pouliasis, E., Di Matteo, P., Haywood, M., A milky way with a massive, centrally concentrated thick disc: new galactic mass models for orbit computations, A&A 598 (2017) A66. doi:10.1051/0004-6361/201527346.
- [24] J. Bovy, Dynamics and Astrophysics of Galaxies, Princeton University Press, Princeton, NJ, (in prep.).
- [25] J. Binney, S. Tremaine, Galactic Dynamics: Second Edition, 2008.
- [26] R. A. Ibata, G. Gilmore, M. J. Irwin, Sagittarius: the nearest dwarf galaxy, Monthly Notices of the Royal Astronomical Society 277 (3) (1995) 781–800. doi:10.1093/mnras/277.3.781.
- [27] M. Bellazzini, R. Ibata, L. Monaco, N. Martin, M. J. Irwin, G. F. Lewis, Detection of the Canis Major galaxy at $(l;b) = (244^\circ; 8^\circ)$ and in the background of Galactic open clusters, Monthly Notices of the Royal Astronomical Society 354 (4) (2004) 1263–1278. doi:10.1111/j.1365-2966.2004.08283.x.

- [28] P. Young, The leapfrog method and other symplectic algorithms for integrating Newton's laws of motion, 2013.
- [29] M. Zemp, J. Stadel, B. Moore, C. M. Carollo, An optimum time-stepping scheme for N-body simulations, *Monthly Notices of the Royal Astronomical Society* 376 (1) (2007) 273–286. doi:10.1111/j.1365-2966.2007.11427.x.
- [30] T. Quinn, N. Katz, J. Stadel, G. Lake, Time stepping n-body simulations (1997). arXiv:astro-ph/9710043.
- [31] C. Dyer, P. Ip, Softening in n-body simulations of collisionless systems, *The Astrophysical Journal* 409 (1993) 60–67. doi:10.1086/172641.
- [32] D. Hestenes, Point groups and space groups in geometric algebra (2002). doi:10.1007/978-1-4612-0089-5_1.
- [33] D. Hestenes, Clifford algebra and the interpretation of quantum mechanics (1986). doi:10.1007/978-94-009-4728-3_27.